The Canadian Mineralogist
Vol. 35, pp. 521-541 (1997)

PETROLOGY OF PICRITIC BASALTS FROM KAMLOOPS, BRITISH COLUMBIA: PRIMARY LIQUIDS FROM A TRIASSIC–JURASSIC ARC

JAMES K. RUSSELL[1] AND LORI D. SNYDER[2]

Igneous Petrology Laboratory, Department of Earth and Ocean Sciences, The University of British Columbia, Vancouver, British Columbia V6T 1Z4

ABSTRACT

The Kamloops Lake picrite suite forms a group of small, isolated outcrops of Triassic–Jurassic volcanic flows, breccias and sills in the Intermontane Belt of south-central British Columbia. They are uniformly olivine-phyric (25–40 vol.%). The phenocrysts are zoned and range in composition from $Fo_{89.3}$ to $Fo_{92.4}$. Augite occurs as a microphenocryst, can be strongly zoned, and has Mg/[Mg+Fe(T)] values of 0.84–0.90. The compositions of clinopyroxene and spinel both suggest crystallization under highly oxidized conditions and overlap compositional fields established for counterparts from arc-related picrites. The whole-rock major-element compositions are rich in Mg (24–34 wt.% MgO), Ni (920–1420 ppm) and Cr (1670–3040 ppm), but show low abundances in all rare-earth elements. Phenocryst abundances, textural features, and variations in major-element compositions suggest significant accumulation of olivine; element-ratio diagrams show that the freshest samples of picrite can be related strictly through olivine sorting. Thermodynamic equilibria are used in conjunction with the measured compositions of olivine phenocrysts to calculate temperature – $f(O_2)$ paths for the primary magmas to the Kamloops Lake picrites. These calculations also demonstrate crystallization under high $f(O_2)$ conditions, such as are found in modern island-arc picritic lavas. On the basis of petrography, mineral and rock compositions and thermodynamic constraints, the Kamloops Lake picrite basalts are presumed to represent primary magmas from a Triassic–Jurassic island arc; melt compositions ranged from 15 to 21 wt.% MgO.

Keywords: picrite, primary magma, primitive, olivine, oxygen fugacity, redox state of iron, island arc, Triassic–Jurassic, Kamloops Lake, British Columbia.

SOMMAIRE

La suite de roches picritiques du lac Kamloops forme un groupe de petits affleurements isolés de coulées volcaniques, de brèches et de filons-couches dans la vallée intérieure de la partie sud-centrale de la Colombie-Britannique. Ces roches sont porphyritiques, à phénocristaux d'olivine (25–40% par volume) zonés ($Fo_{89.3\rightarrow92.4}$). L'augite se présente en microphénocristaux qui peuvent être fortement zonés; leurs valeurs de Mg/[Mg + Fe(T)] vont de 0.84 à 0.90. Les compositions du clinopyroxène et du spinelle indiquent une cristallisation en milieu fortement oxydé, et ressemblent ainsi aux compositions déjà établies dans les suites picritiques d'arcs volcaniques. Les roches sont enrichies en Mg (24–34% MgO, poids), Ni (920–1440 ppm) et Cr (1670–3040 ppm), mais toutes les terres rares y sont présentes en très faibles concentrations. D'après l'abondance des phénocristaux, les textures et les variations en compositions, il semble y avoir eu accumulation de l'olivine. Des diagrammes fondés sur des rapports d'éléments conçus pour tester cette hypothèse montrent que la variation parmi les roches les plus fraîches répond strictement au processus de triage de cristaux d'olivine. Les équilibres thermodynamiques, utilisés avec la composition des phénocristaux d'olivine, ont servi à tracer l'évolution des magmas primaires en termes de température et de fugacité d'oxygène. Ces calculs étayent aussi un milieu de cristallisation à fugacité élevée de l'oxygène, tout comme dans le cas de laves picritiques d'arcs insulaires modernes. Les indices pétrographiques, la composition des roches et des minéraux, et les contraintes thermodynamiques montrent que les basaltes à tendances picritiques de la suite de Kamloops Lake représenteraient des venues de magma primaire contenant de 15 à 21% de MgO dans un arc insulaire d'âge triassique ou jurassique.

(Traduit par la Rédaction)

Mots-clés: picrite, magma primaire, primitif, olivine, fugacité d'oxygène, rapport de Fe^{2+} à Fe^{3+}, arc insulaire, âge triassique–jurassique, lac Kamloops, Colombie-Britannique.

[1] *E-mail address*: krussell@perseus.geology.ubc.ca. On the internet: http://perseus.geology.ubc.ca
[2] *Present address*: Department of Geology, University of Wisconsin at Eau Claire, Eau Claire, Wisconsin 54702, U.S.A.
E-mail address: snyderld@uwec.edu

INTRODUCTION

The Kamloops Lake picrite (KLP) suite comprises a group of small, isolated outcrops of Triassic–Jurassic, porphyritic (olivine ± clinopyroxene) volcanic flows, breccias and sills within the Intermontane Belt of the Canadian Cordillera (Fig. 1). All occurrences are situated within the Quesnellia terrane; Quesnellia is broadly interpreted to comprise remnants of a late Triassic volcanic arc that was accreted onto the western margin of North America in the Late Triassic (Monger *et al.* 1982, Monger 1989). Stratigraphically, the KLP suite appears to overlie rocks of the Triassic Nicola Group (Snyder & Russell 1995) and is, itself, overlain by Eocene volcanic rocks of the Kamloops Group (Ewing 1981a, b, 1982, Snyder & Russell 1995).

In this paper, we present petrographic and chemical data on the Kamloops Lake picrite suite and discuss evidence that these ultramafic rocks crystallized from a high-Mg primary liquid. Furthermore, chemical compositions of rocks and minerals are used to constrain the origin and tectonic affinity of the Kamloops Lake picrite suite. Differentiation of these ultramafic lavas is shown to be satisfactorily modeled by olivine fractionation or accumulation. The compositions of the primary melts for the Kamloops Lake suite and other selected ultramafic suites are estimated from thermodynamic calculations that model chemical equilibrium between the observed composition of olivine and the inferred melt phase. The calculations also elucidate the oxidation state of the ultramafic melt. The Kamloops Lake picrites provide new insight into the nature of mafic– ultramafic magmatism in the Mesozoic island arc setting of Quesnellia.

REGIONAL GEOLOGY

The Kamloops Lake picrite suite crops out at four localities (Fig. 1): near Carabine Creek on the north side of Kamloops Lake (Cockfield 1948), north of Pass Lake near Watching Creek (Cockfield 1948), on an isolated knoll near Jacko Lake one kilometer from the southwestern margin of the Iron Mask batholith (Mathews 1941), and as large screens, rafts and xenoliths within the Iron Mask batholith (Kwong 1987, Snyder & Russell 1995). The exact stratigraphic position of the KLP suite is not certain. The Nicola Group is the most voluminous unit underlying the study area. In the vicinity of Kamloops Lake, it consists of abundant green and red augite porphyry flows and related breccias, bedded and massive tuffaceous siltstones, and minor cherty sediments (*e.g.*, Schau 1970, Preto 1979, Mortimer 1987). The rocks are regionally metamorphosed to the greenschist facies and are, in general, broadly folded, weakly foliated, and cut by prominent northwest-trending structures.

Intruding and overlying the Nicola Group are a variety of intrusive and volcanic rocks. The Iron Mask batholith, a northwesterly trending Early Jurassic (205 ± 4 Ma) composite alkaline intrusive complex, is exposed in the southeastern part of the study area (Preto 1967, Northcote 1977, Kwong 1987, Mortensen *et al.* 1995, Snyder & Russell 1995). It was emplaced along deep-seated northwest-trending structures. Xenoliths of serpentinized picrite are clearly correlative with the KLP on the basis of relict mineralogy, textures and mineral compositions; this correlation establishes the KLP suite of volcanic rocks as older than 205 Ma (Snyder & Russell 1995). The picrite at Carabine Creek is intruded by small granitic stocks belonging to the Copper Creek plutonic suite, which is considered to be post-Early Cretaceous (Cockfield 1948). Eocene Kamloops Group volcanic rocks consist of abundant basalt flows and minor intercalated sediments and overlie much of the study area (Ewing 1981a, b, 1982).

Picrite outcrops are distinctly olivine-phyric and locally have sparse vesicles up to 0.2 cm in size. Commonly, the surfaces of weathered outcrops have a subtle but pervasive knobby, knotted or pitted appearance (1–10 cm scale); this texture is not manifest in any recognizable way on fresh surfaces or in thin section. At Jacko Lake, the texture is pervasive enough to give the picrite outcrops a vague layered appearance. This texture may represent fragmental or brecciated portions of the volcanic units. The picrite located near Watching Creek is distinctly massive; the outcrops are typically dense, black and structureless. The rocks are coarser grained and contain more olivine than at the other localities.

In contrast to these three locations of remarkably well-preserved picrite, exposures within the Iron Mask batholith comprise serpentinized rafts and septa. Primary olivine is commonly preserved, and relict magmatic clinopyroxene also is preserved in some samples. In spite of the alteration, volcanic textures are commonly preserved (Snyder & Russell 1995).

PETROGRAPHY

In thin section, samples of KLP are dominantly olivine-phyric, with subordinate microphenocrystic augite. Most of the picrite samples contain subhedral to euhedral phenocrysts of olivine (Fig. 2a) set in a fine-grained (0.03 mm) volcanic-textured groundmass containing euhedral microphenocrysts of augite (Fig. 2b). Locally (*e.g.*, Carabine Creek), the picrite may contain vesicles (≤0.2 cm) filled with secondary fibrous thomsonite (*e.g.*, Fig. 2a). In thin section, the Watching Creek picrite is coarser grained and texturally is an orthocumulate; large abundant crystals of olivine or partly serpentinized olivine are more or less enclosed by an interconnected network of finer-grained clinopyroxene. The well-developed cumulus texture suggests that the Watching Creek occurrence probably represents a high-level intrusion, although field relationships do not rule out a very thick flow. Detailed petrographic descriptions of these rocks can be found in Mathews (1941) and Cockfield (1948); descriptions of the relict primary magmatic minerals follow.

Olivine

Subhedral to euhedral phenocrysts of olivine range in size from 0.5 to 3.5 mm. The grains show no resorption features, and secondary alteration is commonly confined to the rim and fractures. Abundances of olivine phenocrysts in the Kamloops Lake picrites range from 20 to 30% at Carabine Creek, Jacko Lake and Iron Mask, and from 35 to 50% at Watching Creek. Inclusions of Cr-rich spinel are common. In highly serpenti-

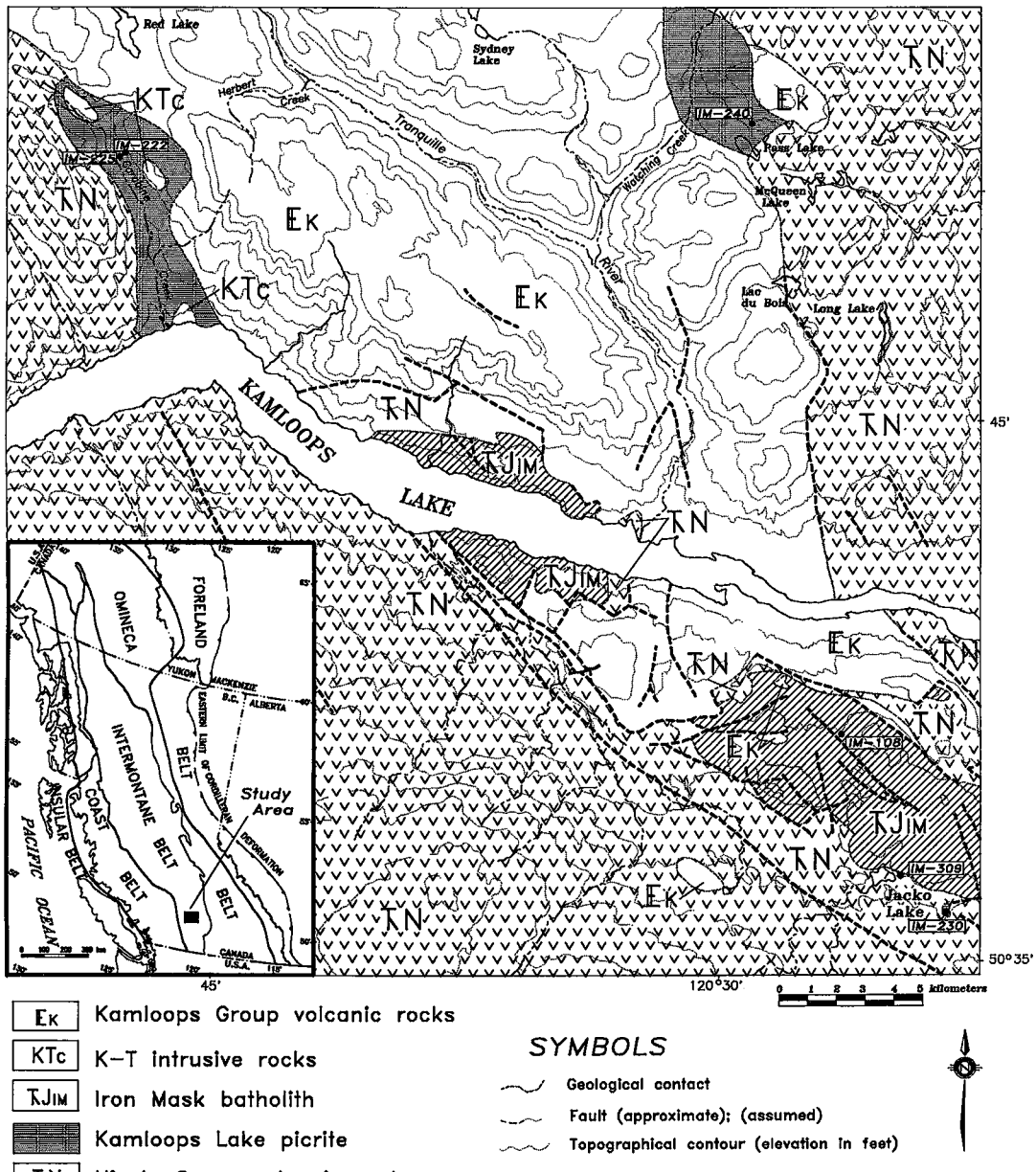

FIG. 1. Geology of the Kamloops Lake area showing picrite occurrences and sample locations. Volcanic and sedimentary rocks of the Nicola Group (Mesozoic) underlie most of the region (after Snyder & Russell 1995).

nized samples (*e.g.*, xenoliths from the Iron Mask batholith), phenocrysts are rimmed by anhedral, fine-grained spinel produced through the oxidation of olivine.

Clinopyroxene

Clinopyroxene occurs as subhedral to euhedral microphenocrysts in picrite from Carabine Creek, Jacko Lake and within xenoliths from the Iron Mask batholith. It shows weak yellow pleochroism. The microphenocrysts are commonly compositionally zoned. At Watching Creek, clinopyroxene is more abundant, occurs as larger grains, and is an intercumulus phase. Inclusions of subhedral to anhedral Cr-rich spinel in clinopyroxene are common in samples from all three localities where unserpentinized material dominates. Pigeonite has been reported at the Jacko Lake locality by Mathews (1941), but none was found during this study.

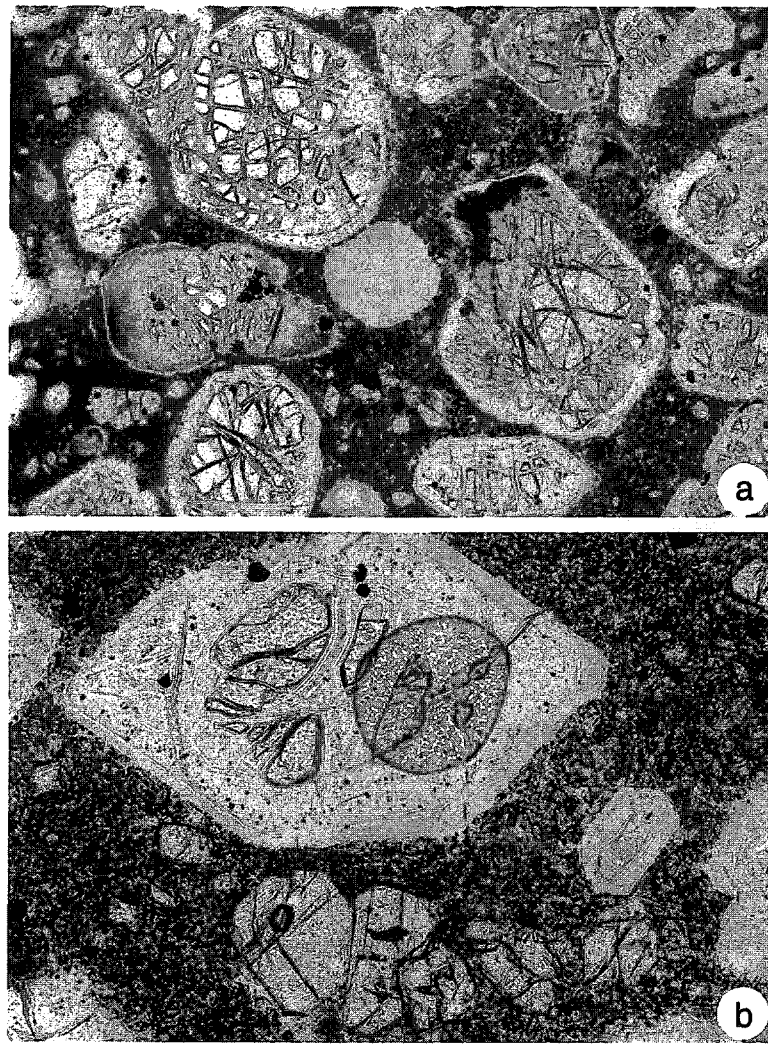

FIG. 2. Photomicrographs of picrite from Carabine Creek locality showing (a) partly serpentinized primary olivine phenocrysts in a fine-grained volcanic matrix, and (b) an isolated pseudomorph of an olivine phenocryst adjacent to smaller crystal of augite. Fields of view are 5 mm and 2.63 mm, respectively.

Cr-rich spinel

Cr-rich spinel in the Kamloops Lake picrites is found as inclusions in olivine and clinopyroxene, as subhedral to anhedral microphenocrysts (up to 0.3 mm) and as subhedral to anhedral crystals (0.05 to 0.15 mm) in the groundmass. Fe–Ti oxides resulting from the secondary breakdown (serpentinization) of olivine and clinopyroxene were not studied in detail nor chemically analyzed (see below).

Mineral Chemistry

Analytical methods

Compositions of olivine, clinopyroxene and spinel were determined using a Cameca SX–50 electron microprobe at The University of British Columbia. Olivine and clinopyroxene compositions were measured using a focused beam at operating conditions of 15 kV and 20 nA for 30 seconds. Background counts were collected for 10 seconds. Standards for olivine include: forsterite (Si, Mg), diopside (Ca), fayalite (Fe), and spessartine (Mn). Standards for pyroxene include: diopside (Si, Mg, Ca), aegirine (Fe, Na) and pyroxmangite (Mn). Spinel analyses were obtained with operating conditions of 20 kV and 30 nA. Standards for spinel analyses include: fayalite (Fe), forsterite (Mg), pyroxmangite (Mn), diopside (Si, Ca), and sphalerite (Zn). A common set of standards was used in the measurement of elemental abundances of Al (grossular), Ti (rutile), Cr (chromite) and Ni (synthetic nickel olivine).

Olivine

Representative compositions of olivine from each of the four localities are given in Table 1. Overall phenocryst compositions define a range $Fo_{89.5–92.5}$ and show slight normal zoning, up to 1 mol.% Fo in samples from Carabine Creek and Jacko Lake. Olivine from the Watching Creek samples is less magnesian and is unzoned, which is consistent with the presence of cumulus textures (*e.g.*, Van Kooten & Buseck 1978).

The minor components are more variable in concentration than Fe and Mg. The Mn content of olivine from the cumulate rocks of Watching Creek ranges from 0.18 to 0.27 wt.% MnO, which is slightly greater than that of olivine from the other three localities (0.08 to 0.21 wt.%). Ca content averages 0.25 wt.% CaO in olivine phenocrysts, and is consistent with an extrusive or hypabyssal environment of crystallization (Simkin & Smith 1970). The Ni content of the phenocrysts ranges from 0.22 to 0.43 wt.% NiO and does not correlate strongly with Fo content (Fig. 3). In terms of both Ni and Fo contents, the olivine compositions are consistent with a mantle-derived origin (*e.g.*, Sato 1977). Also shown for comparison are Ni contents of olivine from other suites of mafic to ultramafic volcanic rocks, including komatiites from Gorgona Island (Echeverria 1980) and the Abitibi greenstone belt (Barnes *et al.* 1983), and picrites from Kilauea (Nicholls & Stout 1988), Baffin Bay (Francis 1985), the New Georgia arc (Ramsay *et al.* 1984) and the Ambae–Vanuatu arc (Eggins 1993). The KLP picrites contain some of the most Ni-rich olivine and match the extreme concentrations of Ni measured for olivine from komatiites and from the Kilauea and Baffin Bay picrites.

TABLE 1. SELECT RESULTS (WT. %) OF ELECTRON-MICROPROBE ANALYSIS OF OLIVINE FROM KAMLOOPS LAKE PICRITES

	Carabine Creek				Watching Creek				Jacko Lake				Iron Mask			
No.	IM224	IM224	IM225	IM225	IM240	IM240	IM241	IM241	IM230	IM230	IM99	IM99	KR07	KR07	KR07	KR07
Spot	c	r	i	r	c	r	c	r	r	c	r	i	c	r	i	r
SiO_2	41.24	41.16	40.83	40.39	39.95	39.66	40.03	40.04	40.80	40.91	40.60	40.74	40.92	40.80	40.79	40.91
Al_2O_3	0.04	b.d.	0.04	0.05	0.05	0.02	b.d.	0.04	0.04	b.d.	0.05	0.03	0.04	0.02	0.05	0.05
Cr_2O_3	0.08	b.d.	b.d.	b.d.	b.d.	b.d.	b.d.	b.d.	b.d.	b.d.	b.d.	b.d.	0.11	b.d.	b.d.	0.08
FeO	6.96	7.66	9.03	8.88	10.07	10.10	10.33	10.07	7.63	7.66	8.84	8.98	7.73	8.92	7.81	7.69
MnO	0.12	0.17	0.18	0.13	0.24	0.22	0.18	0.24	0.11	0.08	0.19	0.17	0.08	0.17	0.13	0.10
MgO	51.25	50.94	49.39	49.19	48.67	48.43	48.82	48.91	50.40	50.22	50.31	49.96	51.37	50.07	51.26	51.71
CaO	0.05	0.06	0.38	0.42	0.28	0.28	0.26	0.25	0.08	0.07	0.29	0.23	0.09	0.18	0.09	0.11
NiO	0.43	0.33	0.22	0.32	0.30	0.31	0.28	0.33	0.41	0.39	0.32	0.34	0.42	0.31	0.28	0.39
SUM	100.17	100.32	100.07	99.38	99.56	99.02	99.90	99.88	99.47	99.33	100.60	100.45	100.76	100.47	100.41	101.04
	Structural formulae calculated on 4 oxygen basis															
Si	0.997	0.997	0.998	0.995	0.988	0.987	0.988	0.987	0.997	1.001	0.988	0.992	0.988	0.993	0.989	0.986
Al	0.001	0.000	0.001	0.001	0.001	0.001	0.000	0.001	0.001	0.000	0.001	0.001	0.001	0.001	0.001	0.001
Cr	0.002	0.000	0.000	0.000	0.000	0.000	0.000	0.000	0.000	0.000	0.000	0.000	0.002	0.000	0.000	0.002
Fe^{2+}	0.141	0.155	0.185	0.183	0.208	0.210	0.213	0.208	0.156	0.157	0.180	0.183	0.156	0.182	0.158	0.155
Mn	0.002	0.003	0.004	0.003	0.005	0.005	0.004	0.005	0.002	0.002	0.004	0.004	0.002	0.004	0.003	0.002
Mg	1.848	1.840	1.800	1.806	1.795	1.797	1.796	1.798	1.836	1.831	1.825	1.815	1.850	1.817	1.852	1.857
Ca	0.001	0.002	0.010	0.011	0.007	0.007	0.007	0.007	0.002	0.002	0.008	0.006	0.002	0.005	0.002	0.003
Ni	0.008	0.006	0.004	0.006	0.006	0.006	0.006	0.007	0.008	0.008	0.006	0.007	0.008	0.006	0.005	0.008
Fo %	92.4	91.9	90.0	90.2	89.7	89.9	89.8	89.9	91.8	91.5	91.2	90.7	92.5	90.8	92.6	92.9

Spot analyses are identified as core (c), interior (i), or rim(r).

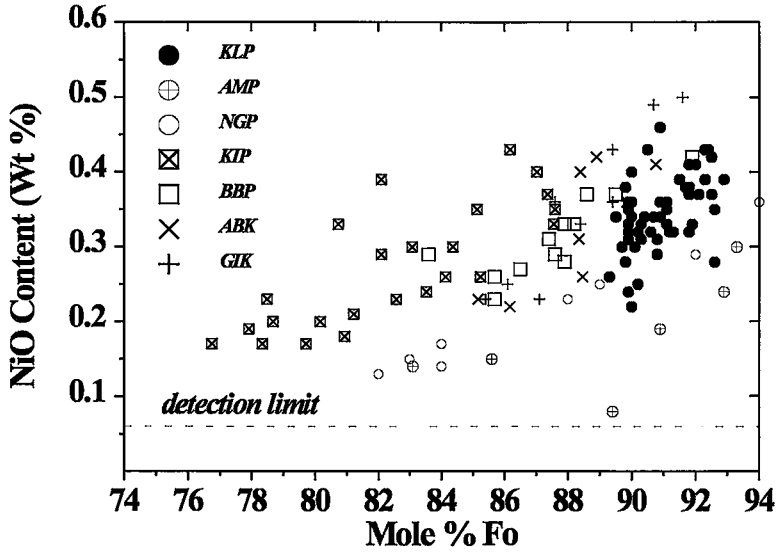

FIG. 3. Ni content of olivine from Kamloops Lake picrite basalts (KLP) and other suites of mafic and ultramafic volcanic rocks, including Ambae (AMP; Eggins 1993), New Georgia (NGP; Ramsay *et al.* 1984), Kilauea (KIP; Nicholls & Stout 1988), and Baffin Bay picrites (BBP; Francis 1985), and komatiites from the Abitibi greenstone belt (ABK; Barnes *et al.* 1983) and Gorgona Island (GIK; Echeverria 1980).

Clinopyroxene

Compositions of representative phenocrysts and microphenocrysts of clinopyroxene are given in Table 2 and plotted in Figure 4. The pyroxene in all cases is augitic; no significant differences exist among or within the four localities. Clinopyroxene grains from Watching Creek exhibit normal zoning from core to rim (up to 5 mol.% Mg), whereas those in rocks lacking a cumulus texture are more strongly zoned, with core-to-rim normal zoning of up to 16 mol.% Fs. Mineral formulae were computed assuming full site-occupancy and charge balance (Table 2), and this required that pyroxene formulae have subequal proportions of Fe^{2+} and Fe^{3+}. In part, the implied high Fe^{3+} content may reflect the fact that the pyroxene crystallized under relatively oxidized conditions (*e.g.*, Barsdell 1988), although it is equally possible that there has been substantial secondary oxidation of the pyroxenes. Furthermore, the estimation of ferric–ferrous iron contents of silicate minerals based on mineral-formula calculations is problematical at best and subject to large errors (*cf.* Luth & Canil 1993, Canil & O'Neil 1996). Consequently, the values of Mg# for pyroxene from the KLP are calculated as $[100 \cdot Mg/(Mg + Fe^{2+} + Fe^{3+})]$. The Mg# values define a range of 84 to 90 (Table 2).

The Cr content of the clinopyroxene ranges from below detection to 1.32 wt.% Cr_2O_3, with an average of 0.66 wt.%. No systematic differences in Cr contents of clinopyroxene are observed between the cumulate and extrusive rocks. Al (1.6–4.7 wt.% Al_2O_3), Ti (0.12–0.44 wt.% TiO_2) and Na (0.17–0.33 wt.% Na_2O) contents of pyroxene are comparable to those of pyroxenes found in island arc picritic suites, such as in Grenada (Arculus 1978), New Georgia (Ramsay *et al.* 1984) and Ambae (Eggins 1993). Clinopyroxene in komatiites from Gorgona Island (Echeverria 1980) and the Abitibi Greenstone Belt (Barnes *et al.* 1983) show a greater range of compositions and can contain more Al.

Cr-rich spinel

Cr-rich spinel from the Kamloops Lake picritic basalts exhibits a wide range of composition (Table 3). Systematic zoning is not observed. The spinel has consistently low Al contents (average 8.4 wt.% Al_2O_3) and variable Cr and Fe^{3+} (Fig. 5). The spinel compositions define two groups, representing cumulate rocks from Watching Creek, which are relatively enriched in Fe^{3+}, and extrusive rocks from the Carabine Creek and Jacko Lake, which are more Cr-rich. The spinel from

TABLE 2. SELECT RESULTS (WT. %) OF ELECTRON-MICROPROBE ANALYSIS OF CLINOPYROXENE FROM THE KAMLOOPS LAKE PICRITES

	Carabine Creek				Watching Creek				Jacko Lake				Iron Mask			
No.	IM224	IM224	IM225	IM225	IM240	IM240	IM241	IM241	IM230	IM230	IM99	IM99	KR07	KR07	KR07	KR07
Spot	Mp-c	Mp-i	Mp-c	Mp-i	Ph-c	Ph-r	Ph-c	Ph-i	Mp	Mp	Mp-c	Mp-i	Mp-c	Mp-i	Mp-i	Mp-i
SiO_2	51.80	50.84	52.01	52.95	51.17	51.15	51.72	49.32	51.07	51.14	51.24	51.98	50.84	52.57	51.52	51.67
TiO_2	0.16	0.25	0.18	0.15	0.20	0.28	0.15	0.41	0.25	0.25	0.19	0.17	0.20	0.14	0.19	0.17
Al_2O_3	2.54	3.26	2.46	1.62	2.97	3.01	2.22	4.32	2.96	2.89	2.79	2.21	3.32	1.94	2.73	2.41
Cr_2O_3	0.94	0.62	0.92	0.85	0.69	0.51	0.77	0.43	0.26	0.26	0.83	0.78	0.98	0.80	0.87	0.80
FeO(T)	4.65	5.39	4.23	3.50	4.98	5.01	4.27	6.02	5.32	5.87	4.71	4.26	4.75	3.93	4.32	4.22
MnO	0.09	0.12	0.06	0.09	0.07	0.07	b.d.	0.12	b.d.	0.14	0.10	0.12	0.08	0.07	0.08	0.08
MgO	16.80	16.05	16.79	17.34	16.55	16.51	17.20	15.64	16.51	16.38	16.74	17.40	16.82	17.98	17.32	17.69
CaO	22.26	22.38	22.52	22.44	22.53	22.40	22.63	22.72	22.17	21.99	22.48	22.35	21.94	21.88	22.34	22.10
Na_2O	0.26	0.28	0.25	0.23	0.29	0.29	0.28	0.27	0.24	0.31	0.28	0.28	0.24	0.22	0.22	0.22
TOTAL	99.50	99.26	99.42	99.17	99.45	99.23	99.24	99.25	98.78	99.23	99.36	99.55	99.17	99.60	99.59	99.36
Structural formulae calculated on 6 oxygen basis																
Si	1.901	1.875	1.909	1.944	1.879	1.882	1.897	1.820	1.888	1.885	1.882	1.900	1.870	1.918	1.883	1.890
Al^{IV}	0.099	0.125	0.091	0.056	0.121	0.118	0.096	0.180	0.112	0.115	0.121	0.095	0.130	0.082	0.117	0.104
Al^{VI}	0.011	0.017	0.015	0.014	0.007	0.012	0.000	0.008	0.017	0.011	0.003	0.000	0.014	0.001	0.001	0.000
Ti	0.004	0.007	0.005	0.004	0.006	0.008	0.004	0.011	0.007	0.007	0.005	0.005	0.006	0.004	0.005	0.005
Cr^{3+}	0.027	0.018	0.027	0.025	0.020	0.015	0.022	0.013	0.008	0.008	0.024	0.023	0.028	0.023	0.025	0.023
Fe^{3+}	0.070	0.096	0.056	0.025	0.103	0.095	0.098	0.154	0.091	0.105	0.100	0.091	0.093	0.066	0.095	0.098
Fe^{2+}	0.072	0.070	0.073	0.082	0.050	0.059	0.033	0.031	0.074	0.076	0.044	0.039	0.053	0.054	0.037	0.031
Mn	0.003	0.004	0.002	0.003	0.002	0.002	0.000	0.004	0.000	0.004	0.003	0.004	0.002	0.002	0.002	0.002
Mg	0.919	0.882	0.919	0.949	0.906	0.906	0.941	0.861	0.910	0.900	0.917	0.948	0.922	0.978	0.944	0.965
Ca	0.875	0.884	0.886	0.882	0.886	0.883	0.889	0.898	0.878	0.868	0.885	0.875	0.865	0.855	0.875	0.866
Na	0.018	0.020	0.018	0.016	0.021	0.021	0.020	0.019	0.017	0.022	0.020	0.020	0.017	0.016	0.016	0.016
Mg#	86.6	84.2	87.7	89.9	85.6	85.5	87.8	82.3	84.7	83.3	86.4	87.9	86.3	89.1	87.7	88.2

Spot analysis labels denote phenocryst (Ph), microphenocryst (Mp) and core, interior and rim.
Mg# = 100*Mg/(Mg+Fe^*).

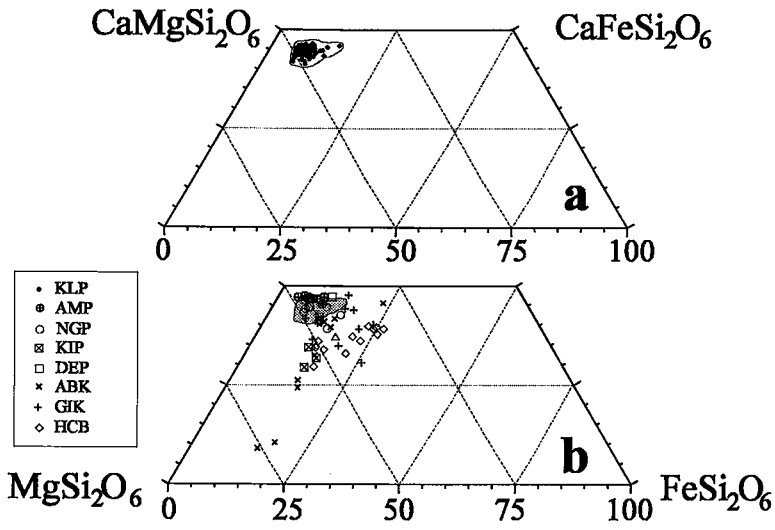

FIG. 4. Pyroxene quadrilateral showing augite compositions from (a) KLP and from (b) other volcanic rock suites (as in Fig. 3). Included are data for Heathcote boninites (HCB; Crawford & Cameron 1985) and Deccan picrites (DEP; Krishnamurthy & Cox 1977).

TABLE 3. SELECT COMPOSITIONS (WT. %) OF SPINELS DETERMINED BY ELECTRON-MICROPROBE ANALYSIS

	Carabine Creek				Watching Creek				Jacko Lake					
No.	IM224	IM224	IM225	IM225	IM240	IM240	IM240	IM240	IM230	IM230	IM230	IM230	IM99	IM99
Spot	Gm	In-ol	In-px	In-ol	Ph-r	Ph-c	In-px	In-px	Ph-c	Ph-i	Gm	Gm	In-px	In-px
SiO_2	0.15	0.06	0.06	0.03	0.04	0.06	0.07	0.04	0.03	0.05	0.56	0.92	0.06	0.74
TiO_2	0.60	0.40	0.58	0.58	1.43	1.16	1.22	1.03	0.48	0.56	0.40	0.72	0.55	0.51
Al_2O_3	8.83	7.17	8.53	8.30	12.08	9.25	8.62	8.63	8.10	8.56	7.16	9.02	7.63	6.94
Cr_2O_3	28.70	49.46	30.60	27.92	10.82	13.65	16.04	15.81	33.75	30.50	32.93	22.45	26.09	27.10
Fe_2O_3	16.00	14.56	15.06	15.57	20.32	19.02	18.62	18.41	14.43	14.95	18.73	19.52	14.88	15.20
FeO	33.22	14.63	32.36	35.32	45.45	46.67	45.31	45.77	30.89	33.91	30.56	37.08	38.34	36.08
MnO	0.43	0.10	0.16	0.21	0.26	0.20	0.23	0.22	0.15	0.17	0.23	0.24	0.20	0.16
MgO	10.83	11.74	11.54	11.21	8.83	9.31	9.58	9.52	12.10	12.03	9.60	9.53	11.50	11.64
CaO	0.09	0.03	0.13	b.d.	0.03	b.d.	0.02	0.02	b.d.	b.d.	0.04	0.08	0.17	0.14
NiO	0.25	0.17	0.28	0.30	0.40	0.39	0.39	0.41	0.29	0.28	0.24	0.31	0.31	0.34
ZnO	0.09	0.10	b.d.	b.d.	b.d.	b.d.	0.09	0.08	0.08	b.d.	0.07	b.d.	b.d.	b.d.
TOTAL	99.19	98.43	99.30	99.44	99.66	99.71	100.19	99.94	100.29	101.01	100.52	99.86	99.73	98.85
	Stuctural formulae calculated on 32 oxygen basis													
Si	0.040	0.016	0.016	0.008	0.011	0.016	0.019	0.011	0.008	0.013	0.151	0.249	0.016	0.201
Ti	0.122	0.081	0.117	0.118	0.291	0.238	0.249	0.211	0.096	0.111	0.081	0.146	0.111	0.104
Al	2.808	2.280	2.699	2.636	3.846	2.972	2.759	2.770	2.535	2.661	2.281	2.873	2.421	2.218
Cr^{3+}	6.123	10.553	6.496	5.950	2.311	2.943	3.444	3.405	7.086	6.361	7.038	4.797	5.555	5.810
Fe^{3+}	6.745	2.971	6.539	7.163	9.240	9.576	9.260	9.381	6.172	6.730	6.216	7.540	7.769	7.362
Fe^{2+}	3.610	3.287	3.380	3.509	4.590	4.338	4.228	4.194	3.203	3.297	4.234	4.410	3.350	3.448
Mn^{2+}	0.098	0.023	0.036	0.048	0.059	0.046	0.053	0.051	0.034	0.038	0.053	0.055	0.046	0.037
Mg	4.357	4.723	4.619	4.504	3.556	3.785	3.879	3.866	4.790	4.731	3.869	3.840	4.617	4.706
Ca	0.026	0.009	0.037	0.000	0.009	0.000	0.006	0.006	0.000	0.000	0.012	0.023	0.049	0.041
Ni	0.054	0.037	0.060	0.065	0.087	0.086	0.085	0.090	0.062	0.059	0.052	0.067	0.067	0.074
Zn	0.018	0.020	0.000	0.000	0.000	0.000	0.018	0.016	0.016	0.000	0.014	0.000	0.000	0.000
Cr#	68.56	82.23	70.65	69.30	37.53	49.75	55.52	55.14	73.65	70.51	75.52	62.54	69.65	72.37
Mg#	54.69	58.96	57.74	56.21	43.65	46.60	47.85	47.97	59.93	58.93	47.75	46.55	57.95	57.71

Labels to spot analyses include phenocryst (Ph), groundmass (Gm) and inclusions (In) hosted by olivine (ol) or pyroxene (px).
Cr# = 100•Cr/(Cr+Al); Mg# = 100•Mg/(Mg+Fe^{2+}).

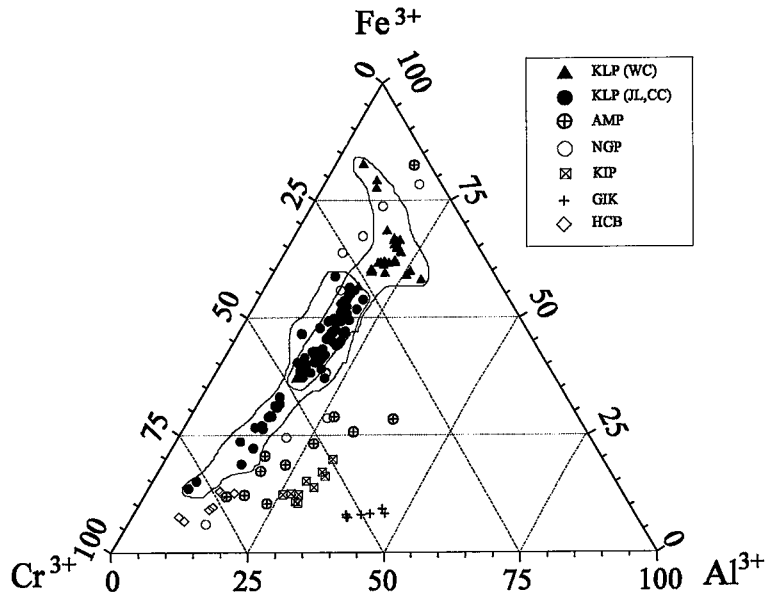

FIG. 5. Compositions of spinel from KLP are plotted in terms of Cr^{3+}, Al^{3+}, and Fe^{3+}. Symbols are used to separate the different occurrences of picrite (Watching Creek *versus* others). Spinel compositions from other suites of volcanic rocks are shown as in Figures 2 and 3.

the cumulate samples also shows higher Ti (0.7 to 3.9 *versus* 0.1 to 0.8 wt.% TiO_2) and Ni contents (0.35 to 0.46 *versus* 0.11 to 0.39 wt.% NiO). Compositions of spinel from other mafic to ultramafic suites (Fig. 5) are similar to the Kamloops Lake rocks, but most suites show slightly higher Al contents. The spinel from komatiites on Gorgona Island (Echeverria 1980) show the greatest concentrations of Al (21 to 26 wt.% Al_2O_3). Spinel compositions from samples of KLP are further distinguished from those found in komatiites by their relative depletion in Zn and Mn (Plaksenko & Smol'kin 1990).

Compositions are plotted as $100 \cdot Mg/(Mg + Fe^{2+})$ *versus* $100 \cdot Cr/(Cr + Al)$ (Fig. 6a) and $100 \cdot Mg/(Mg + Fe^{3+})$ *versus* $100 \cdot Fe^{3+}/(Cr + Al + Fe^{3+})$ (Fig. 6b). Spinel compositions in the KLP suite overlap the fields of spinel from arc-related picrites (*e.g.*, Ramsay *et al.* 1984, Eggins 1993). Furthermore, spinel compositions from the KLP suite are highly oxidized relative to spinel from other common mafic magmas (*cf.* Allan *et al.* 1988); $Fe^{3+}/(Cr + Al + Fe^{3+})$ values range from 0.14 to 0.83 (Fig. 6b). Similar ranges are seen in spinel from picritic rocks in the New Georgia (Ramsay *et al.* 1984) and Ambae–Vanuatu (Eggins 1993) arcs; Ramsay *et al.* (1984) and Utter (1978) argued that highly oxidized spinel compositions, such as these, are restricted to island arc environments. Values of Cr/(Cr + Al) for spinel from the KLP suite range from 49 (Watching Creek) to 71.

Whole-Rock Geochemistry

Major-element variation

Whole-rock compositions for four samples (two from Carabine Creek, one from Watching Creek, and one from Jacko Lake) and two samples of serpentinized picrite collected from screens within the Iron Mask batholith are listed in Table 4. One of the latter samples (IM–108) was analyzed independently six times to establish analytical uncertainty.

The KLP suite is marked by exceptionally low Al (2.17 to 6.84 wt.% Al_2O_3), low Si (38.4 to 43.2 wt.% SiO_2), and very high Mg (24.3 to 33.65 wt.% MgO). The picrites are also markedly low in Ti (0.17 to 0.39 wt.% TiO_2) and Ca (3.2 to 6.0 wt.% CaO). The

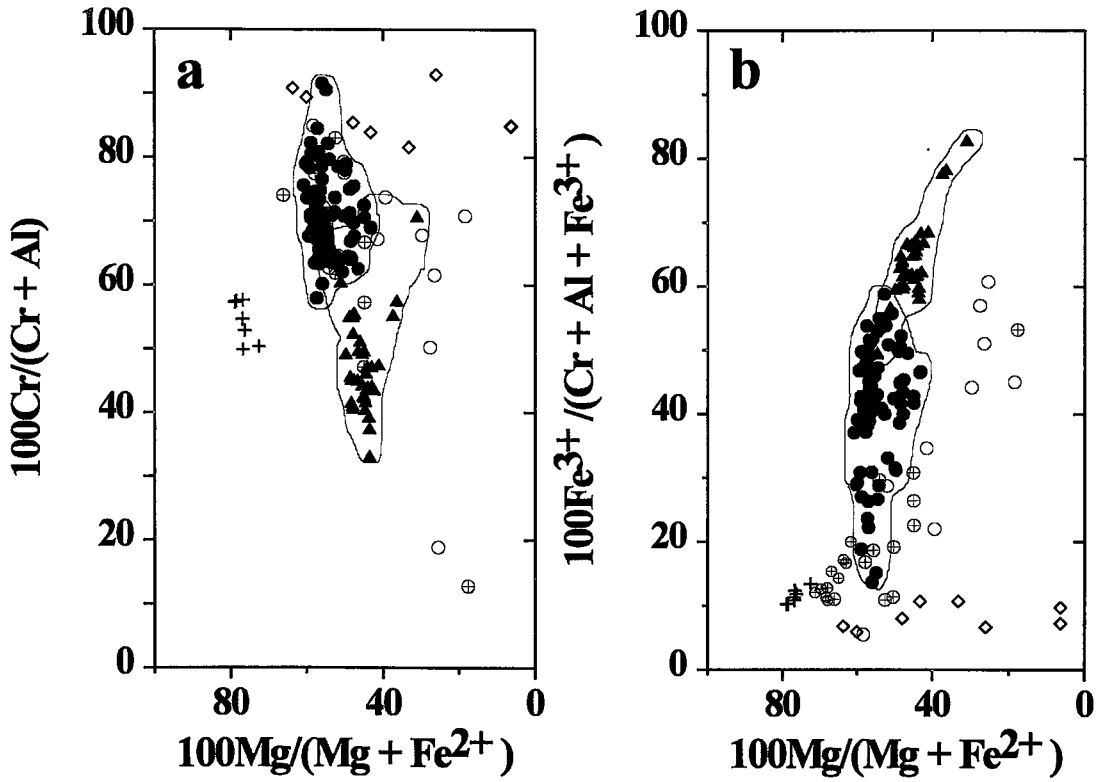

FIG. 6. Spinel compositions (*cf.* Fig. 5) shown as (a) $100 \cdot Mg/(Mg + Fe^{2+})$ *versus* $100 \cdot Cr/(Cr + Al)$, and (b) $100 \cdot Mg/(Mg + Fe^{2+})$ *versus* $100 \cdot Fe^{3+}/(Fe^{3+} + Cr + Al)$.

TABLE 4. MAJOR- AND TRACE-ELEMENT WHOLE-ROCK COMPOSITIONS OF KAMLOOPS LAKE PICRITES

Unit	CC	CC	WC	JL	IM	IM	1s
Sample	IM225	IM222	IM241	IM230	IM108*	IM309	
SiO_2 wt.%	40.40	38.70	38.40	41.30	39.33	43.20	0.197
TiO_2	0.23	0.19	0.17	0.24	0.21	0.39	0.005
Al_2O_3	3.80	3.08	2.17	3.94	2.74	6.84	0.056
Fe_2O_3	5.32	6.42	10.30	4.48	11.00	5.01	0.063
FeO**	3.97	2.64	--	4.72	--	4.40	-
MnO	0.17	0.17	0.18	0.17	0.20	0.14	0.004
MgO	31.40	32.80	32.60	32.30	33.65	24.30	0.217
CaO	4.72	3.20	5.32	4.91	3.53	6.03	0.109
Na_2O	0.09	0.02	0.08	0.18	0.15	0.30	0.012
K_2O	0.95	0.22	0.15	1.50	0.57	2.21	0.012
P_2O_5	0.11	0.10	0.05	0.10	0.06	0.13	0.005
H_2O^+	7.80	11.10	9.20	4.70	7.38	4.80	
CO_2	0.08	0.08	0.36	0.04	0.08	0.03	
SUM	99.04	98.72	98.97	98.58	98.90	97.78	
LOI	8.45	11.80	9.75	4.80	7.10	5.00	
			Trace Elements				
Ba[1] ppm	213	147	226	521	129	354	
Rb[2]	31.1	16[1]	3.8	26.0	16.3	54[1]	
Sr[2]	216.4	122[1]	41.0	112.9	14.0	201[1]	
Nb[2]	0.59	6[1]	0.13	0.37	0.31	3[1]	
Zr[2]	11.8	21[1]	4.4	10.9	10.6	33[1]	
Y[2]	4.34	b.d.[1]	2.57	4.03	3.90	b.d.[1]	
Ni[1]	1350	1380	1420	1410	1254	920	
Cr	2580	3040	2790	2990	2902	1670	
Sc[2]	18.27	14.9[3]	21.41	17.41	20.73	23.6[3]	
Th[2]	0.23	b.d.[1]	0.10	0.27	0.28	b.d.[1]	
U[2]	0.30	b.d.[1]	0.06	0.09	0.20	b.d.[1]	
Hf[2]	0.51	b.d.[3]	0.16	0.44	0.39	0.6[3]	
Co[1]	80	85	87	85	92	66	
Cu[1]	25	15	20	30	25	17	
Ga[1]	16	16	16	16	17	19	
S[1]	b.d.	b.d.	1120	b.d.	1662	b.d.	
Sn[1]	10	10	7	12	4	10	
Zn[1]	58	60	61	60	50	58	

- Localities are Carabine Creek (CC), Watching Creek (WC), Jacko Lake (JL), Iron Mask (IM).
- Major element compositions were determined by XRF analysis at the Department of Earth and Planetary Sciences, McGill University. Analytical methods for trace element determinations include: [1]XRF, [2]ICPMS, [3]Neutron Activation.
*Average of six analyses, **Volumetric Analysis.

rocks are strongly enriched in Ni (920 to 1420 ppm) and Cr (1670 to 3040 ppm) (Table 4). Samples of Kamloops Lake picrites are plotted in Figure 7 on an anhydrous normalized basis. They show relatively low SiO_2 and Al_2O_3 compared to all other suites (Figs. 7a, b) and, with the exception of the komatiites, show the highest contents of Mg. The KLP suite contains similar levels of Ti as found in island arc picrites (*e.g.*, New Georgia and Ambae) (Fig. 7c), is depleted in Ti relative to the Baffin Bay and Kilauea picrites, and is enriched in Ti relative to boninites from Heathcote, Australia (*e.g.*, Crawford & Cameron 1985).

Rare-earth elements

Chondrite-normalized rare-earth-element (REE_{cn}) patterns for the Kamloops Lake picrite suite are shown in Figure 8a, and concentrations are reported in Table 5. *REE* abundances are very low; all normalized values (Boynton 1984) are less than 4, and the patterns are flat. Rocks from the Jacko Lake, Carabine Creek and Iron Mask occurrences have similar profiles. They show slight enrichment of the light rare-earth elements (*LREE*) (La/Sm averaging 1.1) relative to the heavy rare-earth elements (*HREE*) (Nd/Lu averaging 1.4). The serpentinite from the Iron Mask occurrence

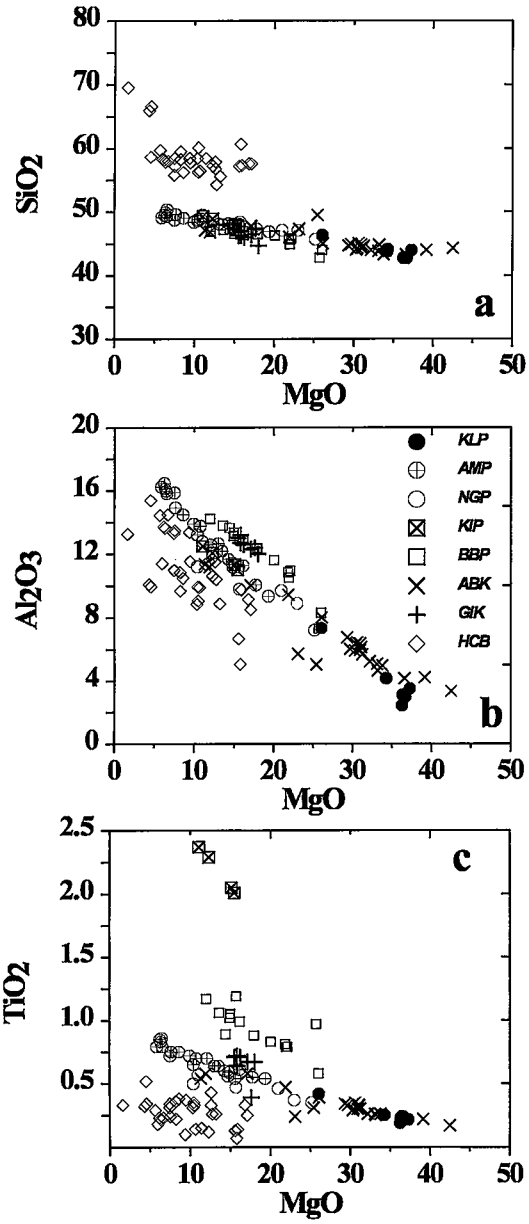

FIG. 7. Normalized chemical compositions of Kamloops Lake picritic basalts and compositions of other suites of volcanic rocks are plotted as: (a) MgO *versus* SiO_2, (b) MgO *versus* Al_2O_3, and (c) MgO *versus* TiO_2. Sources of data: New Georgia (Ramsay *et al.* 1984), Baffin Bay (Francis 1985), Kilauea picrite (Nicholls & Stout 1988), Ambae (Eggins 1993), Deccan (Krishnamurthy & Cox 1977), Gorgona (Echeverria 1980), Abitibi (Barnes *et al.* 1983), Heathcote (Crawford & Cameron 1985), Bonin Island (Hickey & Frey 1982), Vanuatu (Dupuy *et al.* 1982) and MORB (Sun *et al.* 1979).

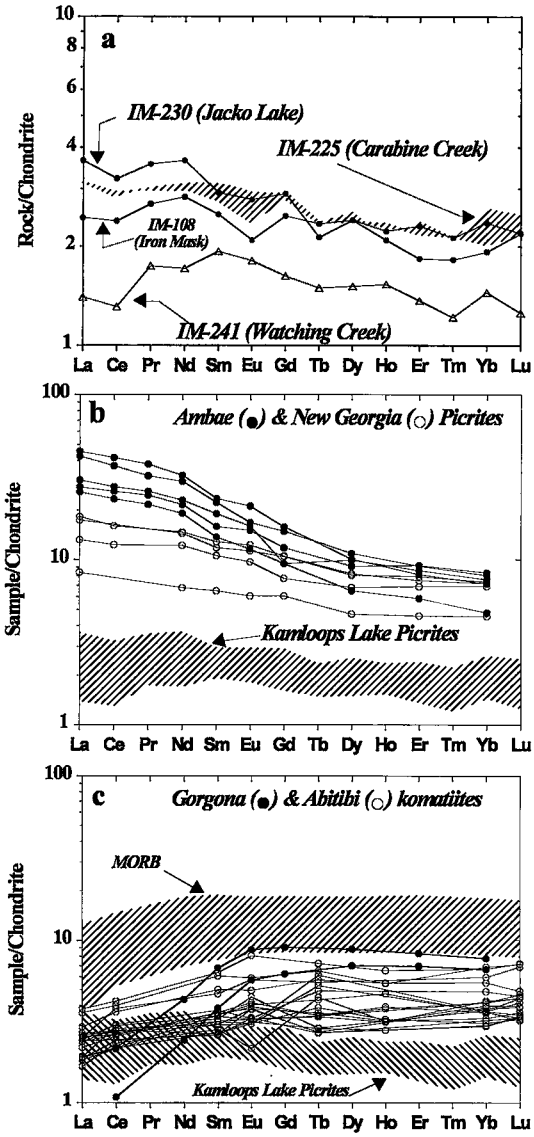

FIG. 8. Chondrite-normalized *REE* patterns for: (a) Kamloops Lake picrites, (b) New Georgia and Ambae picrites, and (c) komatiite suites and MORB. Duplicate analytical data for sample IM–225 are shown as shaded region in (a).

TABLE 5. REE WHOLE ROCK COMPOSITIONS OF KAMLOOPS LAKE PICRITES MEASURED BY INDUCTIVELY COUPLED PLASMA MASS SPECTROMETRY AT THE DEPARTMENT OF GEOLOGICAL SCIENCES, UNIVERSITY OF SASKATCHEWAN

Unit	WC	CC	IM	JL	CC	IM
No.	IM241	IM225*	IM108	IM230	IM222**	IM309**
La	0.44	0.99	0.77	1.15	0.9[1]	2.7[1]
Ce	1.06	2.36	1.94	2.62	b.d.[1]	7[1]
Pr	0.20	0.34	0.31	0.41	--	--
Nd	1.02	1.82	1.69	2.18	b.d.[1]	b.d.[1]
Sm	0.37	0.56	0.48	0.56	0.4[1]	0.9[1]
Eu	0.13	0.19	0.15	0.20	0.2[1]	0.2[1]
Gd	0.42	0.74	0.64	0.75	--	--
Tb	0.07	0.11	0.11	0.10	b.d.[1]	b.d.[1]
Dy	0.49	0.80	0.78	0.78	--	--
Ho	0.11	0.16	0.15	0.16	--	--
Er	0.29	0.48	0.39	0.49	--	--
Tm	0.04	0.07	0.06	0.07	--	--
Yb	0.30	0.48	0.40	0.49	0.3[1]	0.7[1]
Lu	0.04	0.08	0.07	0.07	b.d.[1]	0.11[1]

*Average of two analyses
** Samples analysed by Neutron Activation.

diverges slightly; it has a small depletion in Er and Tm. This divergence may be an expression of *REE* mobility during serpentinization. A consistent feature of the *REE* patterns is a slight depletion in Ce with respect to La, which is typical of island arc suites (Dupuy *et al.* 1982). The samples do not show a significant depletion or enrichment in Eu with respect to Sm and Gd outside of analytical error (shaded area in Fig. 8a), indicating that plagioclase fractionation was not involved in the evolution of these ultramafic lavas.

The cumulate sample from Watching Creek contains significantly lower abundances of the *REE* than the volcanic samples, and has a slightly different pattern. The value of $(La/Yb)_{cn}$ for the Watching Creek sample is 0.97, compared to the range 1.27 to 1.53 established by the three other samples. The overall depleted *REE* profiles of the Kamloops Lake lavas may be accounted for, at least in part, by accumulation of olivine. Indeed, the significantly lower normalized values for all *REE* in the Watching Creek cumulate probably results directly from dilution caused by the greater accumulation of modal olivine.

Figures 8b and 8c show REE_{cn} patterns for other mafic–ultramafic rock suites (*cf.* Table 6). Patterns from island arc suites (Fig. 8b) are enriched in *LREE*, with the Ambae picritic suite (Eggins 1993) showing the greatest enrichment. All of the data for arc picrites show slight depletion in Ce with respect to La, although this feature is not as pronounced as in the Kamloops Lake suite. Absolute *REE* abundances in the New Georgia (Ramsay *et al.* 1984), Ambae (Eggins 1993) and Vanuatu basalts (Dupuy *et al.* 1982) are significantly greater than in the Kamloops Lake rocks. Data for komatiitic rocks of Gorgona Island (Echeverria 1980) and the Abitibi Greenstone Belt (Barnes *et al.* 1983), along with normal MORB (Sun *et al.* 1979), are shown in Figure 8c. These suites show *LREE*-depleted patterns and are relatively lower in absolute abundances than the island arc rocks (Table 6).

The overall flat *REE* pattern of the Kamloops picrites indicates substantial melting in the source region (*e.g.*, Hanson 1980, Dick & Bullen 1984). Experiments have shown that magmas produced by small amounts of mantle melting exhibit *LREE*-enriched patterns, whereas larger amounts of melt (~20% or greater) produce magmas with flat *REE* patterns (Hanson 1989). A simple explanation for the low concentrations and flat *REE* pattern shown by the KLP suite is an origin involving large extents of partial melting of mantle material, with no garnet remaining in the residuum.

TABLE 6. AVERAGE CALCULATED REE_{CN} FRACTIONATION INDICES FOR KAMLOOPS LAKE PICRITES AND FOR OTHER PERTINENT MAFIC AND ULTRAMAFIC VOLCANIC ROCKS, INCLUDING: GORGONA, BARBERTON AND ABITIBI KOMATIITES, NEW GEORGIA AND VANATUA ARC PICRITES AND MORBS (SEE TEXT)

Suite	KLP	Gorgona	Barberton	Abitibi	New Georgia	Vanuatu	MORB
La/Sm	0.9198	0.3012[4]	0.9669	0.6872	1.3659	1.4622	0.6611
Nd/Lu	1.4243	0.4631[1]	1.4521[1]	0.8341[3]	1.8199[1]	1.7830[3]	0.6943[1]
La/Lu	1.2553	0.2222[2]	1.3222[2]	0.5702	2.1771[2]	2.6309	0.5087[2]
No.	4	2	5	23	4	9	5

Other substitute indices were used where data were unavailable: [1]Nd/Yb, [2]La/Yb, [3]Sm/Lu, [4]Ce/Sm.

Incompatible elements

Abundances of incompatible elements are a function of both the source components and fractionation processes and, as such, these patterns can be suggestive of tectonic affinity. Trace-element data for the KLP suite are presented as spidergrams of incompatible elements normalized to primitive mantle (Taylor & McLennan 1985) in Figure 9a, with a field delimiting MORB compositions (Sun *et al.* 1979, Taylor 1980). The Kamloops Lake picritic basalts are depleted, with respect to MORB compositions, in *REE*, Zr, Y and Hf; they are strongly enriched in Rb, Ba, K and, to a lesser degree, Sr, with respect to MORB. The serpentinized sample of picrite from the Iron Mask batholith is aberrantly low in Sr, a feature attributed to secondary alteration.

In Figures 9b and 9c, the trace-element patterns for the KLP suite are compared to data for other mafic–ultramafic volcanic rocks. Figure 9b shows data for modern island arc suites; these patterns are similar to the KLP patterns in that, relative to MORB, they also are enriched in Rb, Ba, K and Sr, and are depleted in Nb. Absolute abundances for most of the incompatible elements in these suites are, in general, slightly greater than the Kamloops Lake picrites, and the intra-suite variation is less pronounced. The modern-day arc rocks are apparently more depleted in Nb and enriched in Ti than the Kamloops Lake suite. One explanation for the lack of a strong Nb anomaly in samples of KLP is that the suite has low *REE* abundances. Therefore, although Nb is strongly depleted with respect to K, the Nb anomaly is not apparent compared to the low La and Ce contents of the KLP rocks. Overall, the Kamloops Lake volcanic suite corresponds best with the trace-element systematics established for modern arc systems (*e.g.*, Perfit *et al.* 1980).

Komatiites from the Abitibi greenstone belt show extreme depletion with respect to K and Sr, but otherwise produce a relatively flat signature (Fig. 9c). Data from picritic basalts from the Deccan flood basalt province (Krishnamurthy & Cox 1977) exhibit a relatively flat, uniform pattern, with only slight relative enrichment in Nb and *REE*.

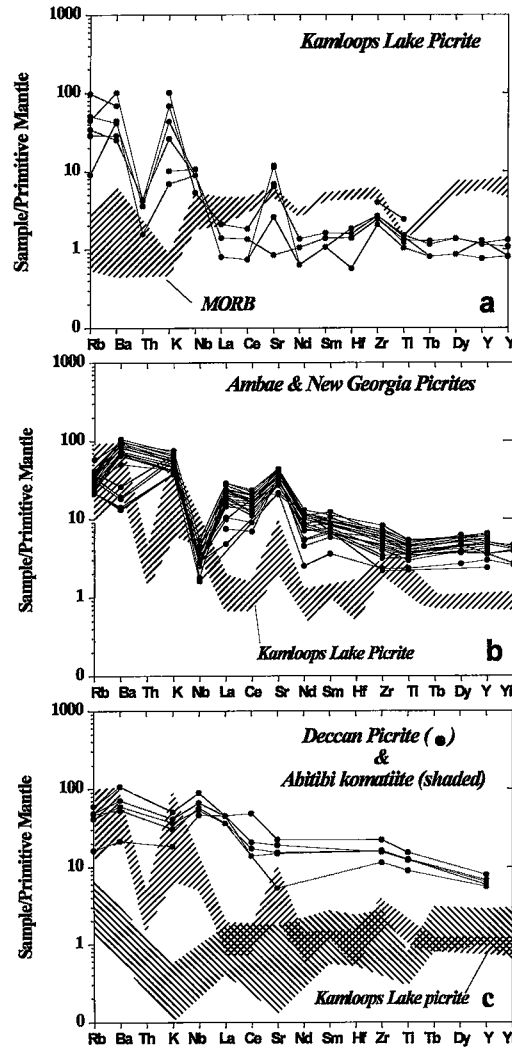

FIG. 9. Normalized concentration-patterns for the incompatible trace elements: (a) Kamloops Lake picritic basalt and MORB, (b) other island-arc rock suites, and (c) Deccan picrites (Krishnamurthy & Cox 1977) and Abitibi komatiites (Barnes *et al.* 1983).

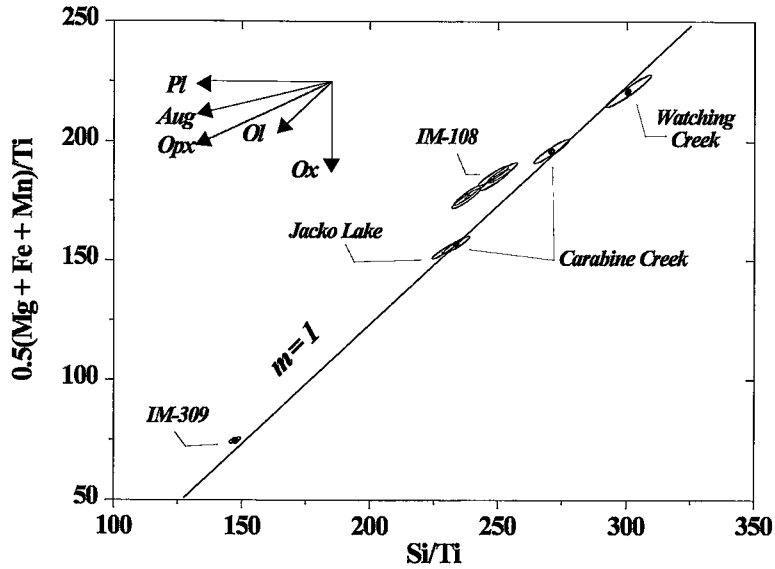

FIG. 10. Pearce-element ratio diagram designed to test the hypothesis that olivine crystallization or accumulation can account for the chemical variation in the Kamloops Lake picritic suite. See text.

MAGMATIC DIFFERENTIATION

An investigation of comagmatic relationships and of processes of magmatic differentiation within the Kamloops Lake picrite suite was undertaken using Pearce Element Ratio diagrams (Pearce 1968, Russell & Nicholls 1988, Nicholls & Russell 1991, Cui & Russell 1995). Diagrams (*cf.* Fig. 10) were designed by choosing an appropriate conserved element as the denominator of the ratio, and choosing a set of numerator elements for the x and y axes that can model the effects of the target mineral assemblage (Stanley & Russell 1989, Nicholls & Gordon 1994). The target mineral assemblage for the Kamloops Lake picritic basalts consists of phenocryst and microphenocryst phases, olivine and clinopyroxene. Titanium was chosen as the denominator element for the Kamloops Lake suite because of low analytical error (Table 4) and the absence of a major Ti-bearing phase in the phenocryst assemblage.

The main concept behind this method is that rocks related to each other through fractionation or accumulation of a given mineral or mineral assemblage will define a line with a predictable slope. For example, Figure 10 contains a diagram designed to test whether compositional variations among picrite samples can be explained by olivine sorting alone. The axes are chosen so that the accumulation or loss of olivine would cause compositions of cogenetic rocks to lie along a line with unit slope. If the picrite occurrences can be related through the fractionation of olivine, then each point should plot along this reference line.

The sample from Carabine Creek (IM–225) was chosen as the reference composition, and a model line (M = 1) was drawn through this data point. It is one of the least altered samples of picrite and has a well-preserved, pronounced volcanic character. The inset vectors in Figure 10 show the competing effects of different magmatic phases; olivine is the only phase that can cause a trend with unit slope by itself. Error ellipses are calculated based on 1σ estimates of analytical error derived from the six replicate analyses of IM–108. Where rock compositions fall within analytical error of the model line, the hypothesis of a cogenetic association cannot be rejected. Compositions that do lie off the model trend do so because a) they are not comagmatic, b) differentiation involved phases other than olivine, c) the magma was affected by mixing or assimilation, or d) the rocks have suffered postmagmatic alteration.

Figure 10 shows that the three localities at which the picrite is relatively unserpentinized can be related through fractionation or accumulation of olivine. The model line drawn through IM–225 intersects (within analytical error) the other Carabine Creek sample, as well as samples from Watching Creek and Jacko Lake. Two samples of serpentinized picrite from the Iron Mask batholith (IM–309, –108) do not fall on the model line, and thus cannot be related simply to picrite from

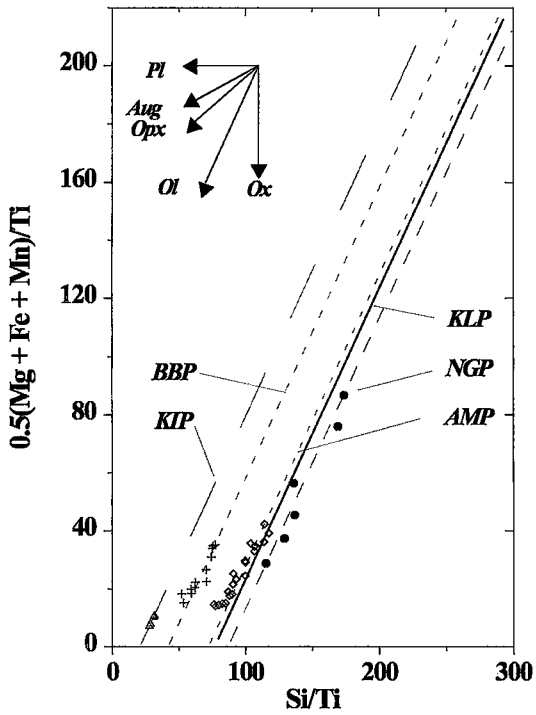

FIG. 11. Several suites of ultramafic rocks are plotted on the same Pearce-element ratio plot as used in Figure 10; a model "olivine-control" line is passed through the most Mg-rich composition of each suite.

other localities. It is likely that the process of serpentinization has caused addition or removal of at least one of the elements used in the diagram (Si, Ti, Mg, Fe or Mn) (Viljoen & Viljoen 1969, Blais & Auvray 1990). If this is the case, comagmatism cannot be discounted.

Several other olivine-phyric mafic–ultramafic rock suites have been plotted on the same olivine "sorting" diagram (Fig. 11). Model olivine-control trends (*e.g.*, M = 1.0) have been projected through the most magnesian sample in each suite. The trend established for the KLP suite (Fig. 10) is shown as a heavy line.

The *y*-intercepts to the model trends on element-ratio diagrams can serve as an important measure of differences in source-region processes (*e.g.*, Nicholls & Russell 1991, Cui & Russell 1995). In a set of samples derived from a single batch of magma and being affected by fractionation of olivine only, a plot of those data on Figure 11 will generate a single linear trend with unit slope (*cf.* Nicholls & Russell 1991). That trend will have a unique *x*-intercept value that relates to the nature of the source region (*e.g.*, enriched *versus* depleted mantle) and the source-region processes (*e.g.*, extent of partial melting: Cui & Russell 1995).

In addition to the trend for the KLP suite, model trends have been constructed for Ambae and New Georgia picrites, Baffin Bay picrites and Kilauea picrites. Each trend generates a unique intercept: –76.7 (KLP), –86.8 (NGP), –72.1 (AMP), –41.9 (BBP) and –20.7 (KIP). Although the intercept values are all different, the arc picrites and the KLP suite have relatively similar values (Fig. 11). The similarity in the intercepts for the Ambae and New Georgia picrites is reasonable in that we expect arc magmas to be generated from similar sources. The intermediate intercept value for the KLP suite strongly corroborates the idea that these are also arc-related picrites.

The Baffin Bay and Kilauea picrites derive from continental and oceanic hotspot magmatism (*e.g.*, Francis 1995). The model intercepts established for these suites are very different from the values established for the arc-related picrites, reflecting the fact that source-region processes in arc systems are significantly different from those characterizing other tectonic environments (*e.g.*, Perfit *et al.* 1980, Dupuy *et al.* 1982, Eggins 1993). Furthermore, the model intercepts discriminate between similar magmatic styles (*e.g.*, hotspots) that have a continental *versus* oceanic association.

SATURATION TEMPERATURE, OLIVINE COMPOSITION AND OXYGEN FUGACITY

Picritic magmas can represent primary mantle-derived liquids or can result from olivine accumulation in basaltic magmas (*e.g.*, Hart & Davis 1979, Elthon 1979, Nicholls & Stout 1988, Francis 1985, 1995). The origin of the Kamloops Lake picrites are somewhat obscured by the fact that the rocks are porphyritic and clearly derive in part from olivine accumulation. However, the presence of euhedral phenocrysts of highly magnesian olivine (*e.g.*, Fo_{88}) with small amounts of normal zoning suggests that these rocks are not far removed from a primary mantle-derived magma. In the following section, we attempt to reconstruct the composition and T–$f(O_2)$ conditions for these mantle-derived island-arc-related liquids.

Model calculations

It is assumed that each sample is, at least in part, the result of olivine accumulation; in principle, each rock can therefore be considered a mixture of the original primary melt and olivine. The recalculation of the primary magma involves simultaneous solution of thermodynamic and mass-balance equations. The first pair of thermodynamic equations ensures equilibrium between the unknown melt phase (*m*) and the observed olivine phenocrysts (*Ol*). The calculated melt phase is an estimate of the original primary melt. Considering a binary solid-solution (Fo–Fa), the thermodynamic constraints are:

$$\mu_{Fo,01} \rightleftharpoons \mu_{Fo,m} \quad (1)$$

$$\mu_{Fa,01} \rightleftharpoons \mu_{Fa,m} \quad (2)$$

The thermodynamic data for these equilibria are taken from Roeder & Emslie (1970). An additional thermodynamic constraint that relates redox state of iron in the melt (*e.g.*, X_{Fe3+}/X_{Fe2+}), oxygen fugacity, and magma temperature comes from the work of Sack *et al.* (1980), Kilinc *et al.* (1983), and Kress & Carmichael (1988, 1991). The coefficients in the equation:

$$\ln[X_{FeO_{1.464}}/X_{FeO}] = 0.232 \cdot \ln f(O_2) + b/T + c \quad (3)$$

are taken from Kress & Carmichael (1988). There is also one mass-balance equation for each oxide constituent (i), thereby ensuring that the moles of each oxide in the cumulate olivine (n_{Ol}) and coexisting melt phase (n_m) balance the oxide abundance in the measured whole-rock (n_{pm}) composition:

$$[n_{pm} \times y_i] = [n_{01} \times w_i] + [n_m \times X_i] \quad (4)$$

where n denotes moles of each phase, and y_i, w_i, and X_i are the respective compositions of the original whole rock, olivine, and the calculated melt phase.

The known variables include the starting bulk composition (y_i) and the composition of the olivine phenocrysts (w_i); calculations used the most Fo-rich composition in each sample. The rock compositions were normalized on an anhydrous basis when converted to mole fractions. The composition of the melt phase (X_i) is an unknown and represents the primary melt. It is essentially the liquid that could be derived from the

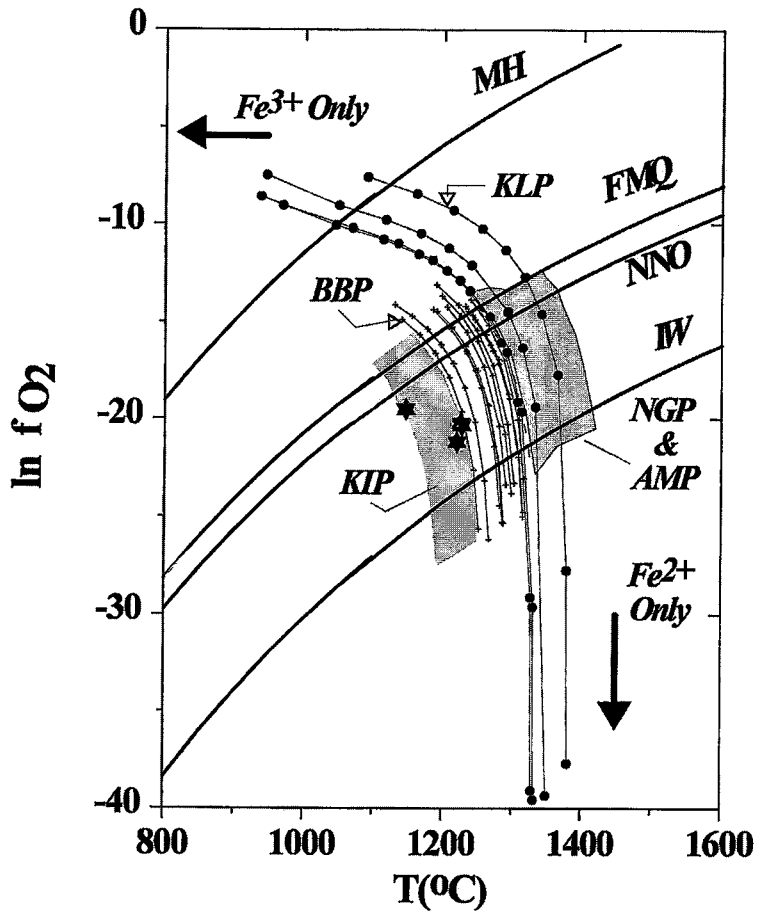

FIG. 12. Model equilibrium rock-paths computed for Kamloops Lake picrites and other mafic–ultramafic volcanic suites and shown as T(°C) *versus* ln $f(O_2)$ (see text).

bulk-rock composition by olivine subtraction and would also be in equilibrium with the observed olivine phenocrysts. Also unknown are the $f(O_2)$ and T of the magma. In many instances, the three thermodynamic equations (Eq. 1–3) and mass-balance relationships (Eq. 4) suffice to solve this problem exactly. In the case of the Kamloops Lake picrites, however, secondary alteration (*e.g.*, groundmass) has modified the original proportion of ferrous to ferric iron in the volcanic rocks. In short, we assume that the total Fe in the original picrite is known, but the original Fe^{3+}/Fe^{2+} is not. This makes one more unknown than there are equations, and thus we can only map out univariant solutions for each rock (Fig. 12).

Operationally, equations 1–4 were solved using the bulk-rock composition adjusted for a variety of Fe^{3+}/Fe^{2+} ratios. The calculations return an equilibrium temperature and oxygen fugacity for the magma, the composition of the coexisting melt phase, and the proportion of olivine (moles per 100 moles) that could be accumulated or fractionated. Repeating the calculations over a range of assumed values of ferric:ferrous ratio defines a path in $T - \ln f(O_2)$ space that is unique for each rock (Fig. 12).

It should be noted that the calculations are performed using only a single composition of olivine, whereas in reality, phenocrysts show a range of compositions. There is also no way to counteract the effects of olivine re-equilibration during or after olivine accumulation (*e.g.*, Van Kooten & Buseck 1978, Nicholls & Stout 1988). In addition, the serpentinites from the Iron Mask batholith have been excluded from model calculations because of the likelihood of major element addition or loss during serpentinization.

Results

The method yields reasonable limits on the conditions of oxygen fugacity, temperature and primary melt composition for the Kamloops Lake picrites. Figure 12 also displays calculated $T - \ln f(O_2)$ rock paths for several other picrite suites; model paths are shown for picrite from New Georgia and Vanuatu–Ambae arcs and for Baffin Bay and Kilauea picrites. Each path represents one rock composition equilibrated with the most magnesian composition of olivine phenocryst over a range of Fe^{3+}/Fe^{2+} (0.004–0.5), which covers most natural systems. The theoretical limits to these paths coincide with compositions where there is either no Fe^{3+} or no Fe^{2+}. The common buffer curves are shown for reference and set reasonable limits on the actual conditions of formation.

The $T - \ln f(O_2)$ paths for the modern-day island arc picrites are represented by a shaded field rather than a set of univariant curves. This is because for several key data-sets, the measured compositions of olivine do not pertain to the same compositions of rock samples. The shaded region represents the limits to rock paths calculated for all New Georgia and Ambae picrites. The rock paths for the KLP suite overlap this field, indicating that the Kamloops Lake picrites originated under similar $T - \ln f(O_2)$ conditions as recorded by primary magmas from modern-day island arcs.

The $T - \ln f(O_2)$ paths computed for the KLP suite and for picrites from modern-day island arcs display consistently greater $f(O_2)$ at a given temperature than do picrites from other tectonic environments. Ballhaus *et al.* (1990) argued that island arc magmas are characterized by higher oxygen fugacities than magmas from most other tectonic environments. For comparison, picrites from Baffin Bay are shown as individual rock-paths, and Kilauea picrites are shown as a shaded field (Fig. 12). Both suites appear to have been generated at relatively lower values of $f(O_2)$ and T. The stars in Figure 12 correspond to individual picrites from Kilauea for which FeO and Fe_2O_3 are measured and are assumed to reflect conditions in the primary magma (*e.g.*, Carmichael 1991). It is interesting to note that the ordering of these five data-sets in terms of $T - \ln f(O_2)$ rock-paths parallels the order of the data-sets shown on element-ratio diagrams (*e.g.*, Fig. 11).

Figure 13 summarizes some of the other variables related to these calculations. In both Figures 13a and 13b, the horizontal axis is the calculated amount of olivine that must be removed from the bulk rock to produce a melt in equilibrium with the observed composition of the olivine phenocryst. In the case of the Kamloops Lake picrites, it roughly measures the extent of olivine accumulation. This variable is plotted against the composition of olivine used in the calculation (Fig. 13a) and against the MgO content of the calculated melt phase (Fig. 13b). Points shown on Figure 12 correspond to the values from Figure 12 that span the IW buffer curve to slightly greater than the FMQ buffer curve, a range of oxygen fugacities that is considered a reasonable estimate of mantle conditions (*e.g.*, Ballhaus *et al.* 1990, Carmichael 1991, Luth & Canil 1993).

The Kamloops Lake picrites, with the exception of some komatiites from the Abitibi greenstone belt, have compositions that require the greatest amount of olivine accumulation (*e.g.*, Fig. 13a). The Watching Creek sample is the extreme of all analyzed samples (Table 7); it requires the accumulation of 65 to 79 moles of olivine per 100 moles of magma. Komatiites from Gorgona Island show the least effects of olivine accumulation, indicating that the olivine found in these samples crystallized from liquids with the same composition as the rocks. In contrast, these calculations suggest that the Kamloops Lake picrites are samples of a partly cumulate portion of the magma chamber.

Calculated compositions of the primary melt and the attendant magmatic conditions for the Kamloops Lake picrites are given in Table 7. Melt compositions are listed for Fe^{3+}/Fe_T values of 0.1 and 0.15. MgO contents in the model liquids range from 16.7 to 20.5 wt.% at an Fe^{3+}/Fe_T ratio of 0.1, and 14.9 to 18.5 wt.% at a ratio

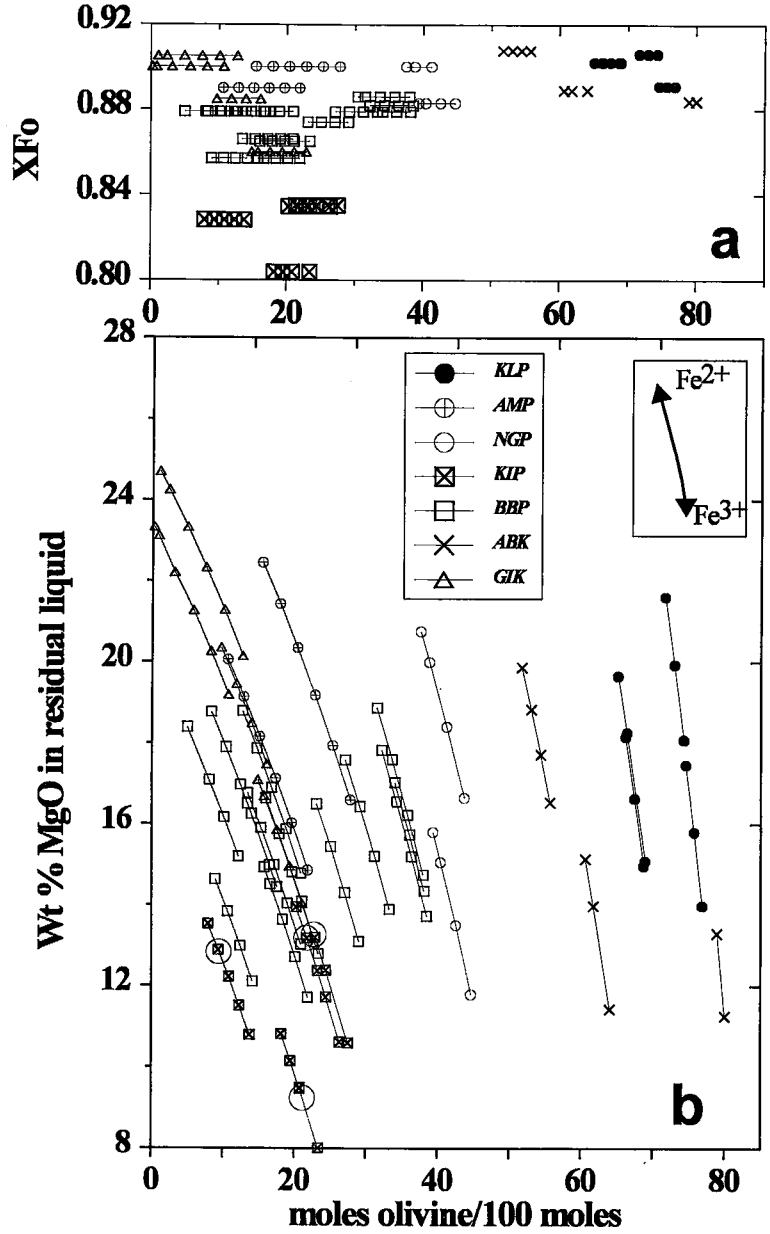

FIG. 13. Model equilibrium rock paths for same data sets as in Figure 12 are summarized as: (a) observed X_{Fo} *versus* calculated olivine accumulation, and (b) calculated MgO content of residual liquids *versus* olivine accumulation (see text).

of 0.15. As Fe^{3+}/Fe^{2+} increases, implied oxygen fugacity increases, equilibrium temperature decreases, and the required composition of the parental melt becomes less magnesian. Although the Kamloops Lake picrite suite has a large amount of accumulated olivine, the calculated compositions of the primary melt are comparable to those found in other primary magmas (*cf.* Elthon 1979, Francis 1985, Nicholls & Stout 1988). The Ambae picrites and the Gorgona komatiites may derive from primary liquids with slightly higher Mg

TABLE 7. CALCULATED MODEL LIQUID COMPOSITIONS AND OTHER PARAMETERS FOR THE KAMLOOPS LAKE PICRITES

Unit	Carabine Creek				Watching Creek		Jacko Lake	
Sample No.	IM225		IM-222		IM-241		IM-230	
X_{Fo} Observed	90.2		90.6		89.1		90.2	
Fe^{3+}/Fe_T	0.10	0.15	0.10	0.15	0.10	0.15	0.10	0.15
$\ln fO_2$	-14.47	-12.91	-13.19	-11.57	-15.03	-13.50	-15.20	-13.58
T (°C)	1293	1264	1325	1295	1271	1241	1275	1243
Olivine Mole %	66	68	72	73	75	76	67	69
SiO_2	50.81	51.78	51.76	52.91	49.12	49.96	50.48	51.43
TiO_2	0.49	0.51	0.50	0.53	0.45	0.47	0.51	0.53
Al_2O_3	6.30	6.61	6.27	6.62	4.57	4.78	6.52	6.83
Fe_2O_3	0.85	1.25	0.91	1.36	0.88	1.29	0.79	1.18
FeO	6.58	5.89	7.08	6.36	6.73	6.00	6.15	5.45
MnO	0.41	0.43	0.50	0.52	0.54	0.57	0.40	0.42
MgO	18.25	16.42	20.45	18.47	16.65	14.92	17.10	15.23
CaO	14.23	14.93	11.84	12.50	20.36	21.30	14.76	15.48
Na_2O	0.25	0.26	0.07	0.07	0.28	0.29	0.49	0.51
K_2O	1.71	1.79	0.48	0.51	0.34	0.36	2.68	2.81
P_2O_5	0.13	0.14	0.15	0.15	0.08	0.08	0.12	0.12
Mg#	0.83	0.83	0.84	0.84	0.82	0.82	0.83	0.83

Mg# = moles MgO/(moles MgO + moles FeO)

contents, up to 23 wt.% MgO for Ambae, and 25 wt.% for Gorgona. Conversely, the Kilauea picrites probably derive from primary magmas with lower Mg contents than those from island arcs.

Conditions of formation

The model melt compositions listed in Table 7 represent our best estimates of the primary melts from which the Kamloops Lake picrites are derived. These estimates of melt compositions have been used in conjunction with the program MELTS (Ghiorso & Sack 1995) to constrain the conditions under which differentiation of these magmas began. Specifically, we have used the compositions of model melts derived for a sample of picrite from Carabine Creek (IM225) as input into MELTS in order to compute P–T liquidus phase-relationships (*e.g.*, Russell & Nicholls 1987, Trupia & Nicholls 1996). The two melt compositions are reported in Table 7 and represent magma compositions assumed to in equilibrium with olivine at different ratios of ferric to ferrous iron.

Figure 14 shows some of the results obtained from MELTS; it can be used to constrain the conditions

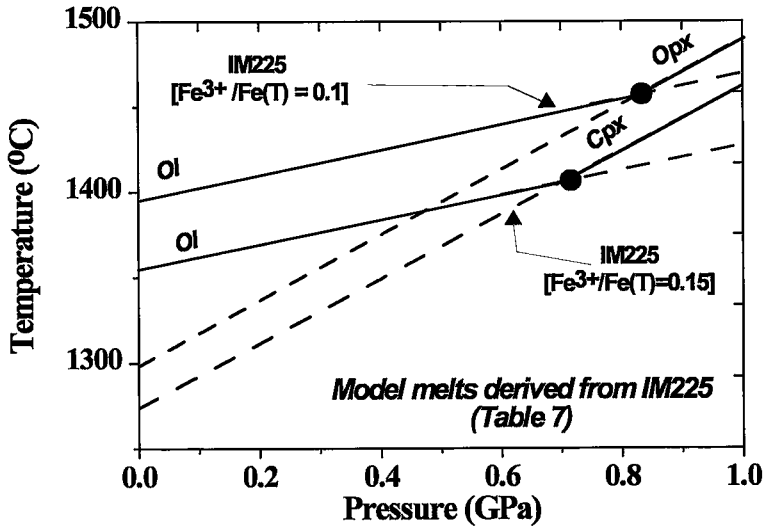

FIG. 14. Calculated P–T phase diagram for model melt compositions derived from sample IM–225 (Table 7) using program MELTS (Ghiorso & Sack 1995). Diagram shows apparent saturation points for olivine and pyroxene (see text).

under which the KLP magmas differentiated. For each of the melt compositions there are two curves, one representing the P–T conditions for olivine saturation, and one representing pyroxene saturation. The phase with the higher saturation temperature at each pressure is taken as the liquidus phase. On this basis, the liquidus surface is mapped by the heavy solid line. Metastable extensions for each phase are shown as dashed lines. The intersection point for each pair of curves denotes the critical pressure (*e.g.*, depth) where the identity of the liquidus phase would change. For example, the less oxidized melt composition [$Fe^{3+}/Fe(T) = 0.1$] is expected to saturate with olivine before orthopyroxene until a pressure of 0.8 GPa, after which orthopyroxene could replace olivine as the early product of crystallization.

Two important insights are gained in Figure 14. Firstly, the picrites record processes of crystallization and crystal accumulation that occurred at a pressure less than 0.7 GPa. The rocks are very olivine-phyric, and contain only microphenocrystic clinopyroxene. Secondly, Figure 14 provides further evidence of the relatively oxidized nature of these magmas. The less oxidized melt [$Fe^{3+}/Fe(T) = 0.1$] appears to favor orthopyroxene as the stable pyroxene phase, whereas at $Fe^{3+}/Fe(T)$ values of 0.15 or greater, the melt saturates with augite after olivine. In all samples that we analyzed by electron microprobe, we found only augite, and never Ca-poor pyroxene.

Summary

The Kamloops Lake picritic basalts represent an episode of mafic to ultramafic volcanism attending the latter stages of Late Triassic Nicola volcanism. Pearce Element ratio modeling indicates that the least-altered samples of the KLP suite could be comagmatic and related through fractionation or accumulation of olivine. The petrography, bulk-rock compositions and mineral chemistry suggest that the KLP are in part cumulate, but retain many attributes of the primary magma. The nature and origins of the primary magmas to the KLP suite have been constrained with thermodynamic calculations. Calculation of $T - \ln f(O_2)$ paths, compositions of the primary melt and extent of "olivine accumulation" indicate that the KLP suite contains a significant cumulate component. Differentiation processes are constrained to have occurred in the crust at pressures less than 0.7 GPa. The calculated rock-paths indicate that the KLP rocks are characterized by crystallization under conditions just as highly oxidized as established for modern-day island-arc ultramafic suites.

Reconstructed primary liquids for the KLP suite range from 16.6 to 20.5 wt.% MgO at $Fe^{3+}/Fe_T = 0.1$ and 14.9 to 18.5 wt.% MgO at $Fe^{3+}/Fe_T = 0.15$, consistent with primary liquids from other localities and tectonic environments. Petrography, mineral and rock compositions, and thermodynamic calculations for the Kamloops Lake picrite suite, suggest that it represents a primary mantle-derived magma formed under highly oxidized conditions. This conclusion is consistent with the KLP suite being part of Quesnellia and representing a portion of an accreted Late Triassic – Jurassic island arc (*e.g.*, Monger *et al.* 1982).

Acknowledgements

Research costs were borne by The Mineral Deposits Research Unit at The University of British Columbia. MDRU received funding in conjunction with the Cu–Au Porphyry Deposits Research Programme, from Natural Sciences and Engineering Research Council of Canada, Science Council of British Columbia, and the following industry sponsors: BP Resources Canada Ltd., Homestake Canada Inc., Kennecott Canada Inc., Placer Dome Ltd., Princeton Mining Corporation, Rio Algom Exploration Inc., and Teck Corporation. We are indebted to Graham Nixon, John Thompson, M. Kopylova, B. Edwards and C.R. Stanley for stimulating discussion and critical comments on early drafts. Careful reviews by Dante Canil and Don Francis benefitted the manuscript immensely, as did editorial work by Graham Nixon and Bob Martin. However, the authors take full responsibility for any residual inconsistencies. This is MDRU publication number 70.

References

Allan, J.F., Sack, R.O. & Batiza, R. (1988): Cr-rich spinel as petrogenetic indicators: MORB-type lavas from the Lamont seamount chain, eastern Pacific. *Am. Mineral.* **73**, 741-753.

Arculus, R.J. (1978): Mineralogy and petrology of Grenada, Lesser Antilles island arc. *Contrib. Mineral. Petrol.* **65**, 413-424.

Ballhaus C., Berry, R.F. & Green, D.H. (1990): Oxygen fugacity controls in the Earth's upper mantle. *Nature* **348**, 437-440.

Barnes S.J., Gorton M.P. & Naldrett, A.J. (1983): A comparative study of olivine and clinopyroxene spinifex flows from Alexo, Abitibi Greenstone Belt, Ontario, Canada. *Contrib. Mineral. Petrol.* **83**, 293-308.

Barsdell, M. (1988): Petrology and petrogenesis of clinopyroxene-rich tholeiitic lavas, Merelava Volcano, Vanuatu. *J. Petrol.* **29**, 927-964.

Blais, S. & Auvray, B. (1990): Serpentinization in the Archean komatiitic rocks of the Kuhmo Greenstone Belt, eastern Finland. *Can. Mineral.* **28**, 55-66.

Boynton, W.V. (1984): Cosmochemistry of the rare earth elements: meteorite studies. *In* Rare Earth Element Geochemistry (P. Henderson, ed.) Elsevier, Amsterdam, The Netherlands (63-114).

CANIL, D. & O'NEILL, H. St. C. (1996): Distribution of ferric iron in some upper mantle assemblages. *J. Petrol.* **32**, 609-635.

CARMICHAEL, I.S.E. (1991): The redox states of basic and silicic magmas: a reflection of their source regions? *Contrib. Mineral. Petrol.* **106**, 129-141.

COCKFIELD, W.E. (1948): Geology and mineral deposits of Nicola map area, British Columbia. *Geol. Surv. Can., Mem.* **249**.

CRAWFORD, A.J. & CAMERON, W.E. (1985): Petrology and geochemistry of Cambrian boninites and low-Ti andesites from Heathcote, Victoria. *Contrib. Mineral. Petrol.* **91**, 93-104.

CUI, Y. & RUSSELL, J.K. (1995): Magmatic origins of calc-alkaline intrusions from the Coast Plutonic Complex, southwestern British Columbia. *Can. J. Earth Sci.* **32**, 1643-1667.

DICK, H.J.B. & BULLEN, T. (1984): Chromium spinel as a petrogenetic indicator in abyssal and alpine-type peridotites and spatially associated lavas. *Contrib. Mineral. Petrol.* **86**, 54-76.

DUPUY, C., DOSTAL, J., MARCELOT, G., BOUGAULT, H., JORON, J.L. & TREUIL, M. (1982): Geochemistry of basalts from central and southern New Hebrides arc: implication for their source rock composition. *Earth Planet. Sci. Lett.* **60**, 207-225.

ECHEVERRIA, L.M. (1980): Tertiary or Mesozoic komatiites from Gorgona Island, Colombia: field relations and geochemistry. *Contrib. Mineral. Petrol.* **73**, 253-266.

EGGINS, S.M. (1993): Origin and differentiation of picritic arc magmas, Ambae (Aoba), Vanuatu. *Contrib. Mineral. Petrol.* **114**, 79-100.

ELTHON, D. (1979): High magnesia liquids as the parental magma for ocean floor basalts. *Nature* **278**, 514-517.

EWING, T.E. (1981a): Regional stratigraphy and structural setting of the Kamloops Group, south-central British Columbia. *Can. J. Earth Sci.* **18**, 1464-1477.

_____ (1981b): Petrology and geochemistry of the Kamloops Group volcanics, British Columbia. *Can. J. Earth Sci.* **18**, 1478-1491.

_____ (1982): Geology of the Kamloops Group near Kamloops. *B.C. Ministry of Energy, Mines and Petrol. Resources, Prelim. Map* **48**.

FRANCIS, D. (1985): The Baffin Bay lavas and the value of picrites as analogues of primary magmas. *Contrib. Mineral. Petrol.* **89**, 144-154.

_____ (1995): The implications of picritic lavas for the mantle sources of terrestrial volcanism. *Lithos* **34**, 89-105.

GHIORSO, M.S. & SACK, R.O. (1995): Chemical mass transfer in magmatic processes. IV. A revised and internally consistent thermodynamic model for the interpolation and extrapolation of liquid–solid equilibria in magmatic systems at elevated temperatures and pressures. *Contrib. Mineral. Petrol.* **119**, 197-212.

HANSON, G.N. (1980): Rare earth elements in petrogenetic studies of igneous systems. *Annu. Rev. Earth Planet. Sci.* **8**, 371-406.

_____ (1989): An approach to trace element modeling using a simple igneous system as an example. *In* Geochemistry and Mineralogy of the Rare Earth Elements (B.R. Lipin & G.A. McKay, eds.). *Rev. Mineral.* **21**, 1-22.

HART, S.R. & DAVIS, K.E. (1979): Nickel partitioning between olivine and silicate melt. *Earth Planet. Sci. Lett.* **40**, 203-219.

HICKEY, R.L. & FREY, F.A. (1982): Geochemical characteristics of boninite series volcanics: implications for their source. *Geochim. Cosmochim. Acta.* **46**, 2099-2115.

KILINC, A., CARMICHAEL, I.S.E., RIVERS, M.L. & SACK, R.O. (1983): The ferric–ferrous ratio of natural silicate liquids equilibrated in air. *Contrib. Mineral. Petrol.* **83**, 136-140.

KRESS, V.C. & CARMICHAEL, I.S.E. (1988): Stoichiometry of the iron oxidation reaction in silicate melts. *Am. Mineral.* **73**, 1267-1274.

_____ & _____ (1991): The compressibility of silicate liquids containing Fe_2O_3 and the effect of composition, temperature, oxygen fugacity and pressure on the redox states. *Contrib. Mineral. Petrol.* **108**, 82-92.

KRISHNAMURTHY, P. & COX, K.G. (1977): Picrite basalts and related lavas from the Deccan Traps of western India. *Contrib. Mineral. Petrol.* **62**, 53-75.

KWONG, Y.T.J. (1987): Evolution of the Iron Mask batholith and its associated copper mineralization. *B.C. Ministry of Energy, Mines and Petroleum Resources, Bull.* **77**.

LUTH, R.W. & CANIL, D. (1993): Ferric iron in mantle-derived pyroxenes and a new oxybarometer for the upper mantle. *Contrib. Mineral. Petrol.* **113**, 236-248.

MATHEWS, H.M. (1941): *Geology of the Ironmask Batholith.* M.Sc. thesis, Univ. British Columbia, Vancouver, British Columbia.

MONGER, J.W.H. (1989): Geology of the Hope and Ashcroft map areas, British Columbia. *Geol. Surv. Can., Maps* **41-1989, 42-1989**.

_____, PRICE, R.A. & TEMPELMAN-KLUIT, D.J. (1982): Tectonic accretion and the origin of two major metamorphic and plutonic welts in the Canadian Cordillera. *Geology* **10**, 70-75.

MORTENSEN, J.K., GHOSH, D. & FERRI, F. (1995): U–Pb geochronology of intrusive rocks associated with copper–gold porphyry deposits in the Canadian Cordillera. *In* Porphyry Deposits of the Northwestern Cordillera of North America

(T.G. Schroeter, ed.). *Can. Inst. Mining Metall., Spec. Vol.* **46**, 142-158.

MORTIMER, N. (1987): The Nicola Group: Late Triassic and Early Jurassic subduction-related volcanism in British Columbia. *Can. J. Earth Sci.* **24**, 2521-2536.

NICHOLLS, J. & GORDON, T.M. (1994): Procedures for the calculation of axial ratios on Pearce element-ratio diagrams. *Can. Mineral.* **32**, 969-977.

_____ & RUSSELL, J.K. (1991): Major-element chemical discrimination of magma-batches in lavas from Kilauea volcano, Hawaii, 1954 – 1971 eruptions. *Can. Mineral.* **29**, 981-993.

_____ & STOUT, M.Z. (1988): Picritic melts in Kilauea – evidence from the 1967–1968 Halemaumau and Hiiaka eruptions. *J. Petrol.* **29**,1031-1057.

NORTHCOTE, K.E. (1977): Iron Mask batholith. *B.C. Ministry of Energy, Mines and Petrol. Resources, Prelim. Map* **26**.

PEARCE, T.H. (1968): A contribution to the theory of variation diagrams. *Contrib. Mineral. Petrol.* **19**, 142-157.

PERFIT, M.R., GUST, D.A., BENCE, A.E., ARCULUS, R.J. & TAYLOR, S.R. (1980): Chemical characteristics of island-arc basalts: implication for mantle sources. *Chem. Geol.* **30**, 227-256.

PLAKSENKO, A.N. & SMOL'KIN, V.F. (1990): Typomorphism of accessory chromian spinels in highly magnesian volcanics. *Int. Geol. Rev.* **32**, 244-259.

PRETO, V.A. (1967): Geology of the eastern part of the Iron Mask batholith. *B.C. Ministry of Energy, Mines and Petrol. Resources, Annual Rep. for 1967*, 137-147.

_____ (1979): Geology of the Nicola Group between Merritt and Princeton. *B.C. Ministry of Energy, Mines and Petrol. Resources, Bull.* **69**.

RAMSAY, W.R.H., CRAWFORD, A.J. & FODEN, J.D. (1984): Field setting, mineralogy, chemistry and genesis of arc picrites, New Georgia, Solomon Islands. *Contrib. Mineral Petrol.* **88**, 3386-3402.

ROEDER, P.L. & EMSLIE, R.F. (1970): Olivine–liquid equilibrium. *Contrib. Mineral. Petrol.* **29**, 275-289.

RUSSELL, J.K. & NICHOLLS, J. (1987): Early crystallization history of alkali olivine basalts, Diamond Craters, Oregon. *Geochim. Cosmochim. Acta* **51**, 143-154.

_____ & _____ (1988): Analysis of petrologic hypotheses with Pearce element ratios. *Contrib. Mineral. Petrol.* **99**, 25-35.

SACK, R.O., CARMICHAEL, I.S.E., RIVERS, M. & GHIORSO, M.S. (1980): Ferric–ferrous equilibria in natural silicate liquids at 1 bar. *Contrib. Mineral. Petrol.* **75**, 369-376.

SATO, H. (1977): Nickel content of basaltic magmas: identification of primary magmas and a measure of the degree of olivine fractionation. *Lithos* **10**, 113-120.

SCHAU, M. (1970): Stratigraphy and structure of the type area of the Upper Triassic Nicola Group in south-central British Columbia. *Geol. Assoc. Can., Spec. Pap.* **6**, 123-135.

SIMKIN, T. & SMITH, J.V. (1970): Minor-element distribution in olivine. *J. Geol.* **78**, 304-325.

SNYDER, L.D. & RUSSELL, J.K. (1995): Petrogenetic relationships and assimilation processes in the alkalic Iron Mask batholith, south-central British Columbia. *In* Porphyry Deposits of the Northwestern Cordillera of North America (T.G. Schroeter, ed.). *Can. Inst. Mining Metall., Spec. Vol.* **46**, 593-608.

STANLEY, C.R. & RUSSELL, J.K. (1989): Petrologic hypothesis testing with Pearce element ratio diagrams: derivation of diagram axes. *Contrib. Mineral. Petrol.* **103**, 78-89.

SUN, SHEN-SU, NESBITT, R.W. & SHARASKIN, A.Y. (1979): Geochemical characteristics of mid-ocean ridge basalts. *Earth Planet. Sci. Lett.* **44**, 119-138.

TAYLOR, S.R. (1980): Refractory and moderately volatile element abundances in the earth, moon and meteorites. *Lunar Planet. Sci. Conf., Proc.* **11**, 333-348.

_____ & MCLENNAN, S.M. (1985): *The Continental Crust: its Composition and Evolution.* Blackwell, Oxford, U.K.

TRUPIA, S. & NICHOLLS, J. (1996): Petrology of Recent lava flows, Volcano Mountain, Yukon Territory, Canada. *Lithos* **37**, 61-78.

UTTER, T. (1978): The origin of detrital chromites in the Klerksdorp Goldfield, Witwatersrand, South Africa. *Neues Jahrb. Mineral. Abh.* **133**, 191-209.

VAN KOOTEN, G.K. & BUSECK, P.R. (1978): Interpretation of olivine zoning: study of a maar from the San Francisco volcanic field, Arizona. *Geol. Soc. Am., Bull.* **89**, 744-754.

VILJOEN, R.P. & VILJOEN, M.J. (1969): The effects of metamorphism and serpentinization of the volcanic and associated rocks of the Barberton region. *Geol. Soc. S. Afr., Spec. Publ.* **2**, 29-53.

Received April 18, 1996, revised manuscript accepted August 20, 1996.